Evaluating adaptation options to sea level rise and benefits to agriculture : the Ebro Delta showcase

Evaluating adaptation options to sea level rise and benefits to agriculture: The Ebro Delta showcase

Ana Genua-Olmedo[1, 3*], Stijn Temmerman[2], Carles Ibáñez[1, 4], Carles Alcaraz[1†]

[1] IRTA, Marine and Continental Waters, Carretera Poblenou km 5.5, 43540 Sant Carles de la Ràpita, Tarragona, Spain

[2] Ecosystem management research group, University of Antwerp, Antwerp 2610, Belgium

[3] Current address: CESAM – Centre for Environmental and Marine Studies, Department of Biology, University of Aveiro, Campus de Santiago, 3810-193 Aveiro, Portugal

[4] Current address: Department of Climate Change, EURECAT, 43870 Amposta, Tarragona, Spain

[*]Corresponding author: agenuaolmedo@gmail.com

[†]Co-corresponding author: carles.alcaraz@irta.cat // carles.alcaraz@gmail.com

Abstract

Sea level rise (SLR) is threatening low-lying coastal areas such as river deltas. The Ebro river Delta (Spain) is representative of coastal systems particularly vulnerable to SLR due to significant sediment retention behind upstream dams (up to 99 %), thereby dramatically reducing the capacity for deltaic sediment accretion. Rice production is the main economic activity, covering 66 % of the delta area, and is negatively affected by SLR because of flooding and soil salinization. Therefore, appropriate adaptation measures are needed to preserve rice production. We combined Geographic Information Systems and Generalized Linear Models to identify zones prone to flooding and increasing soil salinity, and to calculate the so-called sediment deficit, that is the amount of sediment needed to raise the land to compensate flooding and soil salinization. We modelled SLR scenarios predicted by the IPCC Fifth Assessment Report, and analysed the economic feasibility (not the technical feasibility) of reintroducing fluvial sediments retained in the upstream river dam reservoirs into the delta plain, which can contribute to maintaining land elevation and rice production with SLR. To do this, the costs of the sediment reintroduction measures and their benefits in terms of avoided loss of rice production income were evaluated with an approximate economic cost-benefit analysis. Results predicted that between 35 and 90 % of the rice field area will be flooded in the best and worst SLR scenarios considered (SLR = 0.5 m and 1.8 m by 2100, respectively), with a sediment deficit of 130 and 442 million tonnes, with an associated cost of sediment reintroduction of 13 and 226 million €. The net benefit of rice production maintenance was 24.6 and 328 €/ha. The proposed adaptation measure has a positive effect on rice production and can be considered as an innovative management option for maintaining deltaic areas under SLR.

Keywords: climate change; flooding; sediment deficit; rice production; wetlands; coastal adaptation.

1. Introduction

Sea level rise (SLR) is expected to accelerate with global warming through the 21st century (Nicholls and Cazenave, 2010), and is posing a serious threat to low-lying coastal areas, which support about ten percent of the world's population (McGranahan et al., 2007). This situation is especially dramatic in river deltas (Giosan et al., 2014; Tessler et al., 2015), inhabited by more than 500 million people worldwide (Rogers et al., 2013) and which are home to major centres of agriculture (Pont et al., 2002) and other economic activities such as aquaculture and fisheries. River deltas are particularly vulnerable to enhanced rates of relative SLR, as they are often subject to land subsidence, through natural compaction of muddy deltaic sediment deposits and human activities such as groundwater, oil and gas extraction that can further exacerbate subsidence rates (Syvitski et al., 2009; Tessler et al., 2015). The impacts of relative SLR include increasing risks for flood events, coastal erosion, saltwater intrusion into groundwater, habitat and land use changes, and risk of land conversion into permanent open water (Nicholls et al., 2007). These impacts on river deltas are exacerbated by human-driven changes in the river basins (Ericson et al., 2006; Syvitski et al., 2009) such as river channelization, water diversion for irrigation, and damming, which have disturbed the downstream flow of water and sediments, and thereby have altered deltaic environments over the past century (Anthony et al., 2014). Despite dams play a key role in water flow regulation and water scarcity, the blockage of upstream sediment transport causes a reduction in sediment supply to river deltas which has been identified as underlying cause of observed coastal erosion of delta fronts, reduced sediment deposition in deltaic wetlands and thus reduced capacity of deltas to build up with rising sea level (Anthony et al., 2015; Besset et al., 2019; Woodroffe et al., 2006).

Adaptation options such as nature-based solutions are increasingly proposed and investigated in order to restore or facilitate downstream riverine sediment supply, transport, and deposition in delta plains as a potential strategy to adapt and mitigate to SLR effects (Bergillos and Ortega-Sánchez, 2017; Giosan et al., 2014; Temmerman et al., 2013). This concept arose from previously proposed management actions to adapt to SLR in river deltas such as the Mississippi (USA), where since 1900 about 500,000 ha of wetlands have been converted to open water due to submergence by high rates of relative SLR (due to land subsidence) and sediment supply reduction (due to river damming and channelization) (Day et al., 2007). Adaptation options in the Mississippi Delta include the use of dredged sediments for wetland restoration and nourishment, where the dredged sediments are pumped over long distances into the wetlands, and diversion of sediment-rich river water into deltaic wetlands (Day et al., 2005; Peyronnin et al., 2013) although the associated high energy and economic costs, about US$ 40,000/ha (Turner and Streever, 2002). The most cost-effective technique is sediment diversion by reconnecting the river with its deltaic wetlands (Peyronnin et al., 2013), whereas tributary dam bypassing implies a higher cost than building the dams (Kemp et al., 2016). Soft engineering strategies are also applied or proposed in other delta systems: for instance channelization, constructing internal subdeltas, creating new delta lobes in the Danube Delta, Atchafalaya Basin, and Yellow River Delta, respectively (see Giosan et al., 2014); or controlled flooding to allow sediment deposition in the Mekong Delta (HaskoningDHV et al., 2013), and Ganges-Brahmaputra Delta (Auerbach et al. 2015). Other techniques include hydrological restoration by spoil bank removal, or barrier island restoration, which for the Mississippi Delta costs around US$ 3.7 million per kilometre (Day et al., 2005). The implementation of these techniques is expensive, but measures for maintaining deltaic landscapes are needed now in order to avoid costly restoration measures later (Giosan et al., 2014). Besides the long-term benefits, promoting a more natural connection of rivers to delta plain also has an immediate benefit for livelihoods (Darby et al., 2018), for instance in the Mekong Delta sediments provide about half of the nutrients required to sustain rice fields, with a value of $USD 26 million/yr (Chapman and Darby, 2016).

Although adaptation options of river deltas to SLR, through restoring or facilitating riverine sediment supply to the delta plain, is increasingly proposed and discussed in recent literature, relatively few studies have presented a detailed cost-benefit analysis of such adaptation strategies for a specific river delta. Here, the aim of this paper is to evaluate adaptation options to SLR based on fluvial sediment supply measures, for the specific case of the Ebro Delta (Spain). Existing studies on this specific delta have analysed the technical feasibility of implementing adaptation strategies based on reintroducing fluvial sediments into the Ebro Delta plain (*i.e.* Martín-Vide et al., 2004; Rovira and Ibáñez, 2007), but there is no available information about the specific amount of sediment required across the delta and over time to maintain the Ebro Delta elevation under different SLR scenarios. Moreover, a cost-benefit analysis, evaluating the financial costs of introducing fluvial sediments to the delta, against the benefits for society such as maintaining financial income from agricultural production, are lacking. The principal aims of this paper are: (1) to identify areas within the Ebro Delta at risk of flooding under the different SLR scenarios considered; (2) to calculate the volume of sediment deficit under the different SLR scenarios according to the following two considerations: firstly, maintaining the Ebro Delta elevation relative to mean sea level as in the current state (*i.e.* 2010), and secondly, only raising land in the flooded areas and just enough to compensate SLR; and (3) to evaluate the financial costs and benefits (in terms of agricultural income from rice cultivation) of the proposed sediment management measures, and the economic feasibility of implementing them. In this work we analysed the economic feasibility (not the technical/environmental feasibility or ecosystem services) of the adaptation options (*i.e.* reintroducing fluvial sediments retained in the upstream river dam reservoirs into the delta plain). SLR scenarios up to 2100 are selected according to AR5 IPCC projections (Church et al., 2013), and including the upper limit scenario proposed by Jevrejeva et al., (2014).

2. Materials and methods

2.1. Study area

The Ebro River (910 km long) is located in the Northeast of the Iberian Peninsula and drains an area of *ca.* 85,362 km^2. With a mean annual discharge of 426 m^3/s, it is the river with the highest discharge in the Iberian Peninsula. The river flow and sediment transport are modulated by the presence of *ca.* 200 large dams, mainly built for hydroelectricity and irrigation purposes. In the lower Ebro River, the construction of two large dams in the 1960s, Mequinensa and Riba-Roja (*ca.* 100 km upstream from the river mouth, Figure 1), have modified the downstream river flow and sediment transport. Consequently, present river discharge is *ca.* 30 % lower than original, and *ca*. 99 % of the sediment is retained behind the dams (Rovira and Ibáñez, 2015). Hence, this leads to a dramatic reduction in sediment deposition in the delta plain. Thus, the delta is no longer able to grow both seaward and vertically, and suffers from an intense reshaping of the coastline by wave erosion (Sánchez-Arcilla et al., 2008). Coastal deposits are mainly composed of fine sand (particle diameter <0.2 mm), and the delta plain of silt and clay (≤0.062 mm) (Martín-Vide et al. 2004). These particles can be transported by discharges from 10 to 25 m^3/s and discharges from 70 to 170 m^3/s can transport in suspension particles of 0.3 mm (Martín-Vide et al. 2004; Rovira and Ibáñez, 2007). The Ebro Delta, with a surface area of about 320 km^2, is one of the largest deltas in the NW Mediterranean Sea. It is a low-lying area characterized by an elevation gradient from a maximum of *ca.* +5 m above mean sea level (AMSL, referred to mean sea level in Alicante datum) close to the river bank, down to the coastline. Close to 50 % of the total delta surface is below +0.5 m AMSL (Figure 1). At the coast, the tidal range is very small, *i.e.* on average only 16 cm (Cacchione et al., 1990). The Ebro Delta supports a high diversity of ecosystems (*e.g.* wetlands and lagoons), waterfowl and wildlife, as well as socio-economic activities such as rice agriculture, tourism, fishing and aquaculture. Rice is the predominant crop (Figure 1), with an area of *ca.* 210 km^2 (66 % of the total deltaic surface) and an average production of *ca.* 6339 kg per hectare (MAGRAMA, 2017). Fresh water from the Ebro River is diverted to the rice fields by gravity from a weir located 60 km upstream from the river mouth, and it is transferred by two irrigation channels that run parallel to the river course and branch into a network of irrigation channels spreading out over the delta plain (Figure 1).

2.2. Flood model

The Ebro Delta areas at risk of flooding due to different SLR scenarios (see section 2.6 below) were determined in a Geographical Information System (GIS) environment (ArcGIS 9.3) by using a Digital Elevation Model (DEM) based on elevation data from 2010 (hereafter referred to as the reference state). The DEM (Figure 1), with a spatial resolution of 1×1 m and a height accuracy of 15 cm, was developed by the Cartographic and Geological Institute of Catalonia (ICGC) using LIDAR technology. Elevation data were referred to mean sea level in Alicante datum. The Ebro Delta habitats were classified according to the CORINE Land Cover Mapping (Bossard et al., 2000) (Figure 1), and were then reclassified in two categories: (1) rice fields (covering up to 66 % of the delta), and (2) other deltaic areas including saline vegetation (*e.g. Phragmites spp.* and *Salicornia spp.*), other crops (e.g. arable and woody crops), sandy coastal and beach habitats. Cartographic databases were also used to identify delta areas connected to water bodies (*e.g.* sea/river/lagoons).

In each modelled step, every cell elevation located below mean sea level was initially classified in two categories: (1) below mean sea level with direct connection to water bodies; and (2) below mean sea level without direct connection to water bodies. For modelling purposes, both categories were merged since in unconnected cells below mean sea level, flooding due to rise of groundwater is expected and the number of unconnected cells was negligible compared to those from the first category. Hence flooding depth under different SLR scenarios is simply modelled as the projected future sea level minus the reference soil elevation in each cell of the DEM. Tidal effects were not considered since the small average tidal range of 16 cm is in the same order as the estimated maximum vertical error of 15 cm on the DEM.

2.3. Estimation of the sediment volume deficit

The volume of sediment that would be needed to build up land with rising sea level (further referred to as the sediment volume deficit, m^3) was spatially calculated in the Ebro Delta. Two different scenarios were modelled: Scenario 1 (SC1) considered the total volume needed to maintain the deltaic surface elevation relative to mean sea level as in the reference state; and Scenario 2 (SC2) considered the total volume needed to raise land only in the flooded areas and just enough to compensate SLR. Thus, the sediment volume deficit is calculated as follows:

SC1: $V_i = SLR_i \times A$

SC2: $V_i = (SLR_i - Zpixel_{i-1}) \times A \quad \text{for} \; Zpixel_{i-1} \leq SLR_i$

, where V_i is the sediment volume deficit (m^3) in a given modelled time step *i*, SLR_i is the amount of sea level rise (m) at time *i*, A is the pixel area (m^2), and $Zpixel_{i-1}$ is the pixel elevation (m) from the Digital Elevation Model in the time step prior to *i*. The equations above calculate the sediment volume deficit per pixel of the DEM, and then is summed over all pixels over the whole delta.

2.4. Sediment transport and economic cost

The adaptation strategy of extracting and introducing fluvial sediments was evaluated following the technical studies of Martín-Vide et al., (2004) and Roca and Martín-Vide (2005). Briefly, these studies considered the extraction of fluvial sediments from the Riba-Roja Reservoir (see Figure 1), and its transport and deposition in the Ebro Delta rice fields, as a countermeasure against the relative SLR. The sediment transport consisted in two parts: (1) first, from the reservoir to the Xerta weir (Figure 1) by using different engineering techniques; and then (2) from the Xerta weir to the rice fields via the rice irrigation network (Figure 1) and the river's transport capacity. In the first part, three engineering techniques were considered to extract the sediment from the reservoir to the Xerta weir: mechanical dredging (solid material is extracted using a spoon dredge), suction dredging (sediment is extracted with a pump), and flushing (a flow peak is used to mobilize sediment due to the force of the water), see Blazquez et al., (2001), Harvey et al., (1998) and Ji et al., (2011) for more details.

In the case of both mechanical and suction dredging, once the sediment is extracted from the reservoir, the sediment requires an extra transport to arrive to Xerta weir. This extra transport has an additional economic cost, and we considered three different ways: by a pipeline, by boat or by trucks. For modelling purposes and to simplify the results, we only considered the cheapest extra transport (*i.e.* by pipeline, 1.4 €/m^3 of sediment) and discarded the transport by boat (2.3 €/m^3), and by trucks (12.2 €/m^3). In case that boat and truck transport would be considered, one would only have to add their additional cost (0.9 and 10.8 €/m^3, respectively) to the estimated total cost (Table 1). In terms of economic cost, flushing has no additional cost to transport the sediment from the reservoir to the weir when compared to mechanical and suction dredging (Table 1).

2.5. Economic cost-benefit analysis:

The economic cost-benefit analysis considered the financial cost of the implementation of the sediment extraction and transport techniques based on our estimations of the sediment volume deficit (€/m^3) versus the financial benefits of maintenance of rice production in the Ebro Delta. These benefits were based on the models of rice production under different SLR scenarios developed in our previous study (Genua-Olmedo et al., 2016). Briefly, we established a significant negative relationship between soil salinity and rice production in the Ebro Delta, and subsequently modelled the spatial variations (with a 1 × 1 m resolution) and temporal variations (up to 2100) in soil salinity and related rice production under different SLR scenarios (RCP 4.5 and RCP 8.5). Since rice production varies year by year due to climatic factors, data from local farmers were normalized in a rice production index (RPI). RPI ranged from 0 (minimum rice production, 5,814 kg/ha) to 100 (maximum rice production, 10,073 kg/ha). From each scenario of rice production, the estimated income from rice production (in €/ha) was calculated by converting RPI to rice production (kg/ha) according to the following equation: rice production = 5,814 + (10,073 – 5,814) × RPI, and then multiplying rice production by 0.28 €, the price per kilogram of rice paid to farmers in the Ebro Delta. In the present study, we modelled soil salinity, rice production index, and income under different SLR scenarios following the models in Genua-Olmedo et al., (2016), and considering the two approaches of sediment volume deficit (explained in section 2.3). The models in Genua-Olmedo et al., (2016) did not consider adaptation scenarios. We compared the rice income values with and without adaptation. The net benefit of the adaptation strategy of introducing fluvial sediments for a given scenario was calculated by the difference between the rice income with the adaptation (*i.e.* sediment deposition to compensate for the sediment volume deficit), and the rice income without adaptation (without sediment deposition). The cost was calculated by the cost of sediment extraction and transport based on our estimations of sediment volume deficit (explained in section 2.3 and 2.4). Finally, the economic cost-benefit analysis was the difference between the benefit and the cost.

2.6. Bulk density and organic matter estimation

In order to enable calculation of the sediment mass that needs to be extracted and transported from the reservation, the sediment volume deficit (V, m^3) was converted to sediment mass deficit (S, kg) by using the following equation: $S = V \times BD$, where BD is the dry bulk density (kg/m^3). Several studies have shown that bulk density of deltaic sediments is highly related to sediment organic matter content (Curtis and Post 1964; Périé and Ouimet, 2008), thus, in order to assess this relationship in the Ebro Delta, we gathered data of bulk density and organic matter content from 25 rice fields sampled between 2015 (15) and 2016 (10), and 35 wetlands sampled in 2009 (11) and 2015 (24). Different regression models between sediment dry bulk density and organic matter content were tested (see Supplementary Table 1), and finally a modified logarithmic function from Périé and Ouimet (2008) was selected. Model selection was done following the criterion of maximization of Pearson's correlation coefficient between observed and predicted values of bulk density (Figure 2). The selected regression equation was:

$BD = -0.970 + 1.033 \times OM - 0.912 \times \ln(OM) - 0.095 \times [\ln(OM)^2]$; Pearson's $r = 0.86$, $N = 125$, $P < 0.0001$

, where BD is the bulk density (g/cm^3), and OM is the organic matter content (g/g soil).

In order to build an OM spatial distribution model, we obtained data from 900 different rice fields (Figure 1), sampled by the "Agrupacions de Defensa Vegetal of Catalonia" during the 2003–2007 period. The relationship between OM and soil descriptors (see Supplementary Table 2) was analysed with Generalized Linear Models (GLMz). An information-theoretic approach was used to find the best approximating models following the methodology described by Burnham and Anderson (2002). GLMz were built including all possible combinations of independent variables, excluding interactions due to the large number of variables included. Two additional criteria were used to define the best candidate models: (1) only those models performing significantly better than the null model (*i.e.* the model including only the intercept), by a likelihood-ratio test, were considered, and to avoid multicollinearity effects (2) models with a variance inflation factor (VIF) > 5 were not selected (Brockwell and Davis, 2002; Maggini et al., 2006). The degree of support of each candidate model was assessed with the second order Akaike Information Criterion (AICc); and then AICc was rescaled to obtain ΔAICc values ($\Delta AICc = AICc_i$ – minimum AICc). For the current analysis we examined in detail the set of models with $\Delta AICc \leq 4$, since models with $\Delta AICc > 4$ have less support and might be omitted from further consideration. Then, the relative plausibility of each candidate model was assessed by calculating Akaike's weights (w_i); w_i ranges from 0 to 1, and can be interpreted as the probability that a given model is the best model in the candidate set.

Because no model was clearly the best one (*i.e.* $w_i \geq 0.9$), we calculated model-averaged regression coefficients (β_i) by weighing selected model coefficients by model w_i. The relative importance of each variable was also calculated by the sum of w_i for all models in which a given variable occurs, which estimates the importance of an independent variable for differentiating the response variable (see Burnham and Anderson, 2002). Finally, model-averaged estimates were compared with regression coefficients from the full model to assess the impact of model selection bias on parameter estimates (Whittingham et al., 2005). For all of the candidate models the full model residuals were tested for normality through the Shapiro-Francia normality test; the residuals of all models were normally distributed ($P \geq 0.20$). Prior to analysis, quantitative variables were log-transformed to improve linearity and homoscedasticity. All statistical analyses were performed with R software version 3.6.3 (R Core Team 2016); MuMIn 1.43.15 was used for multi-model inference analysis; car 3.0-7 was used for VIF analysis of each of the candidate models; and Nortest 1.0-4 was used for normality test analysis.

Model efficiency was quantified with the Pearson's correlation coefficient between observed and predicted values. The calibration process mostly consisted in optimizing regression models (GLMz) by introducing and deleting different model parameters (see Supplementary Table 2) to maximize Pearson's r values. Optimization of the fit eliminated most of the over-prediction. Model selection and calibration (Figure 2) were done with 75 % of the data, and the remaining data (25 %) was used for model validation.

2.7. Sea level rise scenarios

The flooded area, sediment volume deficit and associated cost of sediment supply (*i.e.* extraction and transport), and economical benefit of rice production maintenance were modelled under different SLR scenarios based on the projections of the Fifth Assessment Report (AR5) carried out by the IPCC, the Intergovernmental Panel on Climate Change (Church et al., 2013). Representative Concentration Pathways (RCPs) are different greenhouse gas (GHG) concentration trajectories adopted by the IPCC for AR5 modelling and used for climate change research. RCPs provide a quantitative description of concentrations of GHG emissions measured in CO_2 equivalents in the atmosphere over time, as well as their radiative forcing up to 2100 (Van Vuuren et al., 2011). Two RCPs were selected: the RCP 4.5 (stabilization) and RCP 8.5 (increasing radiative forcing). The former is a mitigation scenario, with an emissions peak around 2040 and then declining resulting in a mean global temperature increase of +2.4 ºC and mean SLR averaged over 2081 to 2100 of +0.47 m. The latter is a 'business as usual' scenario with emissions continuing to rise through the 21st century, resulting in a mean global temperature increase of +4.3 ºC and mean SLR averaged over 2081 to 2100 of +0.63 m (Church et al., 2013). Following Jevrejeva et al., (2014) we also included a worst case SLR scenario (called upper limit, hereafter), with a 5 % probability of being exceeded, resulting in a mean SLR by 2100 of +1.80 m. Model simulations were obtained for 2010 (reference state), 2025 and from 2030 to 2100 in 10-year steps (Supplementary Table 3).

3. Results

3.1. Flood model

The flood simulations identified the areas of the Ebro Delta prone to be flooded under the considered SLR scenarios if no adaptation measures are implemented. As expected, a progressive inundation of the rice fields and natural habitats was predicted up to 2100 (Figure 3). The inundation process started in lowland areas connected to water bodies (*e.g.* sea/river/lagoons), whereas the last flooded areas were those located along the river, characterized by higher elevations (Figure 3; Supplementary Table 4; Supplementary Figure 1). For the RCP 4.5 scenario, the flooded area showed a progressive increase over time reaching a maximum of 140 km^2 (or 44 % of the total delta surface) by 2100. For the RCP 8.5 scenario the inundation process was faster and the flooded area varied between 145 and 240 km^2 (or 45 and 75 % of the total delta area) for the mean and upper limit SLR scenario, respectively (Figure 3; Supplementary Table 4). By 2100, the potential loss of rice field area (*i.e.* loss is considered as soon as rice fields are below mean sea level) ranged between 35 and 90 percent depending on the considered scenario (Figure 3; Supplementary Table 4). Results also showed that for the mean and high SLR RCP 4.5 scenarios, about 25 percent of the rice fields would be below sea level by 2080 and 2060, respectively. For the mean, high and upper limit SLR RCP 8.5 scenarios, it would happen by 2070, 2060 and 2040, respectively (Supplementary Table 4). For the other deltaic areas (*e.g. Phragmites spp*, wetlands, dunes and beaches) the relative area loss (*i.e.* when the land elevation becomes below mean sea level) up to 2100 varied between 37-66 % depending on the considered scenario. The period in which about 25 percent of the other deltaic areas (*i.e.* natural environments) would be flooded was reached in 2060 and 2050 for both RCP 4.5 scenarios, and in 2060, 2050 and 2040, for mean, high and upper limit SLR RCP 8.5 scenarios, respectively (Supplementary Table 4).

3.2. Bulk density and organic matter

Bulk density (BD) showed a spatial distribution within the Ebro Delta, with the highest values close to the shoreline and along the Ebro River bank (Supplementary Figure 2). Lower values were found around the coastal lagoons and the freshwater springs. The mean value of BD was 1.00 g/cm^3, being 0.93 g/cm^3 in rice fields, with a range from 0.69 to 1.15 g/cm^3. Wetlands showed a smaller BD mean of 0.74 g/cm^3. BD was strongly negatively related to organic matter (OM) content (Supplementary Figure 2). The results of the information-theoretic analysis provided predictive models of the effect of the analysed variables on the spatial distribution of soil OM content (Table 2). The correlation between observed and predicted values was statistically significant (Pearson's r = 0.80, N = 455, P < 0.0001), supporting the predictive ability of the model (Figure 2). According to the AICc selection process (*i.e.* ΔAICc ≤ 4) only one model was considered as plausible (Table 2). Among the variables in the model (Supplementary Table 2), only six of the variables initially included were selected: Euclidean distance to the inner border, Euclidean distance to the mouth, surface elevation, the quadratic component of Euclidean distance to the coast, soil salinity, and surface elevation (Table 2). The mean value of OM was 0.03 g/g soil (Supplementary Figure 2), with a range of 0.01–0.07 g/g soil in rice fields, and 0.01–0.25 g/g soil in wetlands.

3.3. Estimation of sediment volume deficit

We estimated the sediment volume needed to compensate the sea level rise in the Ebro Delta for both SLR RCP 4.5 and RCP 8.5 scenarios. Results of the SC1 approach (maintaining surface elevation relative to mean sea level as in the reference state) showed that the total average sediment volume deficit in the Ebro Delta rice fields (for the period 2010-2100) ranged between 122×10^6 m^3 and 418×10^6 m^3 depending on the considered SLR scenario, while in the whole delta ranged between 156×10^6 m^3 and 534×10^6 m^3 (Supplementary Table 4). In the SC2 approach (sediment volume needed to raise flooded land just enough to compensate the SLR), the sediment deficit showed a spatial gradient with the lower values along the river and the highest nearby the coastline and coastal lagoons, following the surface elevation gradient (Figure 1; Figure 4). Based on the considered SLR RCP scenario, the sediment volume deficit in the rice fields ranged between 24.8×10^6 m^3 and 227×10^6 m^3, for the period 2010-2100, while in the whole delta this was between 33.7×10^6 m^3 and 298×10^6 m^3 (Supplementary Table 4). In both SC1 and SC2 approaches, the sediment volume deficit showed a non-linear increase over time, following a sigmoidal trend that was more apparent in the upper limit SLR scenario (Figure 5; Supplementary Table 4). The difference in sediment deficit between SC1 and SC2 in the rice fields ranged between 97.2×10^6 m^3 and 191×10^6 m^3 by 2100, depending on the evaluated SLR RCP scenario, whereas in the whole delta the difference in sediment deficit between SC1 and SC2 ranged between 122×10^6 m^3 and 236×10^6 m^3. In SC1, by 2100, the annual sediment deficit rate (*i.e.* the sediment addition that would be necessary) for the whole delta ranged between 1.7×10^6 m^3 and 6×10^6 m^3, whereas in SC2 this ranged between 0.4×10^6 m^3 and 3.3×10^6 m^3, depending on the considered SLR scenario.

3.4. Economic cost-benefit analysis: sediment supply cost vs rice production benefit

The economic cost-benefit analysis considered the cost of both sediment extraction and transport (Table 1) based on our estimations of the sediment volume deficit in SC1 and SC2, and the benefits of rice production maintenance (*i.e.* the normalized rice production index, RPI) in the Ebro Delta. In both scenarios, the net benefit was the difference between the rice income with the adaptation (sediment deposition), and the rice income without adaptation (without sediment deposition). In SC1 (*i.e.* introducing the sediment volume needed to maintain deltaic surface elevation relative to SLR), the mean normalized rice production index by 2100 was 61.2 % with a mean income of 2,359 €/ha/yr, *i.e.* the same value as in the reference state, since delta land elevation is maintained along the 21st century (Figure 4; Supplementary Table 4). In SC2 (*i.e.* considering the sediment needed to raise inundated areas just enough to compensate SLR), a progressive soil salinization was predicted leading to a reduction in RPI and consequently in income. Thus, the RPI decreased from 61.2 % to a range from 56.7 to 52.6 % by 2100, depending on the SLR scenario considered, representing an economic loss (income reduction) ranging from 55 €/ha to 104 €/ha (Figure 6; Supplementary Table 4). Compared to SC1, in the SC2 there was a total income reduction in rice production of 2,184,000 € by 2100. When no adaptation was considered the total income reduction was 6,888,000 € by 2100.

Regarding the costs, among the three considered techniques to extract the sediment (*i.e.* mechanical dredging, suction dredging and flushing), flushing was by far the cheapest (Figure 7, Table 1, Supplementary Table 5). Furthermore, mechanical and suction dredging presented extra costs associated with the sediment transport (Table 1), and both techniques were very similar in average cost (Figure 7). To compensate the sediment deficit in rice fields, the flushing technique showed a cost variation in SC1, by 2100, from 66 million € (for RCP 4.5 mean SLR scenario) to 226 million € (for the RCP 8.5 upper limit SLR scenario), whereas for the same SLR scenarios, in SC2 the cost ranged from 13 to 122 million €, respectively (Figure 7). Thus, by 2100, the annual cost was 733,333 €/yr and 144,444 €/yr in SC1 and in SC2, respectively for the RCP 4.5 mean SLR scenario and, 2.5 and 1.4 million €/yr in SC1 and SC2 respectively for the RCP 8.5 upper limit SLR scenario. By contrast, the mechanical dredging, considering the average of the maximum and minimum cost value, showed a cost variation in SC1 by 2100 from 1,123 million € to 3,827 million €, according to considered SLR scenarios (Figure 7, Supplementary Table 5). In SC2, by 2100, for the same SLR scenarios, the average cost ranged between 227 to 2,074 million €. The economic cost-benefit analysis, namely the difference between the benefit and the cost, showed a negative balance in all scenarios (Supplementary Table 6). The most optimal balance was obtained by using flushing to compensate the sediment deficit in SC2. Despite the reduction in rice production in SC2, the lower sediment requirements reduced the total costs, thus the economic cost-benefit balance was optimal when compared to SC1.

4. Discussion

4.1. Assessment of flooding with SLR and model limitations

Our modelling approach allows to identify the areas within the Ebro Delta that are prone to flood risks induced by the different SLR scenarios, in case that no sediment deposition would take place, essentially accounting for the spatial variations in land elevation within the delta plain. Depending on the considered SLR scenario, between 35 and 90 % of the rice field area (which covers today 210 km^2) would be below mean sea level by 2100. Sea flooding and the sediment deficit will affect the integrity of the shoreline since it leads to a reduction in sediment deposition in the delta, as well as wave induced erosion. This does not necessarily mean that rice cultivation would stop in areas below sea level (some present-day rice fields in the Ebro Delta are indeed cultivated below mean sea level), but increasing costs of maintenance and decreasing rice production can make rice production economically unfeasible in the lowest areas (López-Dóriga and Jiménez, 2020). The effect, as barriers, of current human infrastructures (*e.g.* roads, buildings, irrigation network) were included in the flood model. In the Ebro Delta there are no man-made coastal defences such as dykes or embankments, thus, the construction of these coastal defences can be considered as an adaptation measure to reduce the impact of SLR. However, this classical engineering approach (*i.e.* business as usual approach) consisting in impounding low-lying areas prone to flooding or erosion with hard defence structures presents high economic and energetic costs (Day et al. 2005), and do not avoid salt intrusion (Genua-Olmedo et al., 2016).

One of the model limitations is that delta subsidence process has not been included due to the lack of reliable data. Although different estimates are available, with a maximum of *ca.* 2.7 mm/year (Rodríguez-Lloveras et al., 2020), there are no spatially explicit data available yet. As such, one could say that model results are rather conservative. On the other hand, we included extreme SLR scenarios up to 1.8 m by 2100 (Jevrejeva et al., 2014). Furthermore, we estimated sediment deficit considering the maximum subsidence rate (*i.e.* 2.7 mm) reported in Rodríguez-Lloveras et al., (2020) in order to assess the worst possible situation. Considering this subsidence rate, the sediment volume deficit in SC1, by 2100, increased from 122 (without subsidence) to 179×10^6 m^3 (for RCP 4.5 mean SLR scenario), and from 418 to 474×10^6 m^3 (for the RCP 8.5 upper limit SLR scenario), whereas for the same SLR scenarios, in SC2 the sediment volume deficit increased from 24.8 to 53.8×10^6 m^3 and from 227 to 279×10^6 m^3, respectively (Supplementary Table 7). Accordingly, there is an increase in the cost of sediment extraction by flushing of 31 and 29 million €, in both SC1 and SC2 respectively (for the RCP 8.5 upper limit SLR scenario), and 509 and 178 million €, by mechanic dredging.

Another limitation is that our modelling approach does not account for the natural capacity of deltaic habitats, such as beaches and wetlands, to adapt their elevation to SLR by enhanced sediment accretion (Gedan et al., 2011; Kirwan et al., 2016; Schuerch et al., 2018). In this respect, the loss of rice fields depends on the distance to the coast, because, assuming the dynamic nature of the coastal response to SLR, beaches and dunes can serve as protective barriers against flooding since they have a certain capacity to maintain their elevation relative to sea level rise through natural processes of sand accretion (Warren and Niering, 1993). However, most of the Ebro Delta coast is currently retreating (Sánchez-Arcilla et al., 2008), which is aggravated by the dominance of sediment transport by waves due to the reduction of sediment supply by the river discharge (Jiménez and Sánchez-Arcilla, 1993). Furthermore, there are rice fields located along the inner bays (see Figure 1), where beaches are absent and where rice fields cannot count on the protection by beaches and dunes. Thus, rice cultivation may become unsustainable and a conversion into saline wetlands is expected (Fatorić and Chelleri, 2012). Such wetlands could trap sediments and improve the quality of water draining from the rice fields by creating green filters, and as such build up land with SLR and serve as natural protective barriers for inland rice fields (Kirwan and Megonigal, 2013; Temmerman and Kirwan, 2015). Wetlands have already been constructed with this purpose in the Ebro Delta (see http://www.lifeebroadmiclim.eu/en/), but their capacity for vertical accretion, carbon sequestration and nutrient removal is still being assessed. In the Ebro Delta, previous results on vertical accretion in constructed wetlands have been obtained in small experimental plots, with accretion rates higher than 1 cm/yr (Calvo-Cubero et al., 2013), which is in balance with a present-day relative SLR rate of 1.1 cm/yr (Church et al., 2013).

4.2. Dealing with the sediment deficit

The volume of the estimated sediment deficit by 2100 in SC1 (the scenario considering the volume needed to maintain deltaic surface elevation relative to mean sea level as in the reference state) varied for the entire delta between 156×10^6 m^3 in the most conservative SLR scenario (mean RCP 4.5, SLR = 0.5 m), and 534×10^6 m^3 in the worst case SLR scenario (upper limit RCP 8.5, SLR = 1.80 m). These values decreased in the SC2 (considering the total volume needed in the inundated areas, just enough to compensate the SLR) to 34×10^6 m^3 and 300×10^6 m^3 in the most conservative and worst case SLR scenario, respectively. The annual sediment deficit by 2100 for a SLR of 0.5 m was 1.73×10^{6} tonnes/yr and 0.38×10^{6} in SC1 and SC2, respectively. These findings seem to be consistent with previous studies that have estimated the sediment deficit in the Ebro Delta ranging from 1.3×10^{6} to 2.1×10^{6} tonnes/yr under relative SLR of 0.70 m (Ibáñez et al., 1997). However, the annual sediment deficit ranges between 3.3×10^{6} and 6.0×10^{6} tonnes/yr in our estimations for a SLR of 1.8 m. This range is higher due to the more than one meter of SLR difference in comparison with the SLR considered in Ibáñez et al., (1997).

To compensate the sediment deficit in the Ebro Delta, the following adaptation measure is being considered: restoring part of the sediment flux of the lower Ebro River by extracting fluvial sediments from the Riba-Roja reservoir, and transporting the sediment from the reservoir to the Xerta weir by using engineering techniques, and then, from the Xerta weir to the rice fields by using the rice irrigation network. Of the three engineering techniques considered (mechanical dredging, suction dredging and flushing, Table 1) flushing is the cheapest option and according to Roca and Martín-Vide (2005) is the most suitable measure in mobilizing the sediment. Successful removal of reservoir sediment has been applied worldwide (see Kondolf et al., 2014 for an extensive review) such as in reservoirs of Cachí, Costa Rica (Jansson and Erlingsson, 2000); Halligan, United States (Wohl and Cenderelli, 2000); and Hengshan and Zhuwo, China (Wang and Chunhong, 2009).

This study presents an analysis of the sediment volume that would be needed to compensate relative SLR, and it evaluates the financial costs against the benefits in terms of rice production income. However, it does not include a feasibility study on the distribution of sediments by controlled river flood pulses, neither a hydrodynamic or sediment transport model, to evaluate whether sediments can be indeed distributed via the network of irrigation channels towards the rice fields, and subsequently trapped and deposited on the rice fields to meet the spatial patterns of sediment volume deficits as identified in our study (Figure 4). The cost of transporting the different sediment fragments is expected to be different and the volume of water for natural transport varies significantly, coarser sediment fractions require higher river discharge for sediment transport initiation. Also, a previous study of the sediment quality (*i.e.* pollution and contamination) should be considered. Thus, further feasibility studies are needed in the Ebro Delta to investigate which controlled river discharge pulses are needed and feasible to realize enough sediment transport capacity to distribute and deposit sediments over the whole delta in order to compensate for relative SLR. Such a feasibility study for the Ebro Delta, could follow examples of studies on sediment redistribution in the Mississippi Delta (Day et al., 2003; Day et al., 2018), where controlled diversions of river water are implemented to deliver sediments to the deltaic wetlands at large scales, in order to stimulate wetland sedimentation and elevation gain with relative SLR.

Compared to a scenario of no adaptation to SLR, the application of the considered adaptation measure (*i.e.* introducing fluvial sediments) reduced soil salinity, thus minimizing the loss of rice production and economic income. Comparing both sediment addition scenarios (SC1 and SC2), the loss of income in the most conservative scenario (RCP 4.5, SLR = 0.5 m) by 2100 is *ca.* 55 €/ha higher in SC2 than in SC1. Thus, considering the 21,000 ha of rice fields, this represents a total of 1,155,000 € accumulated until 2100. In the most extreme scenario (RCP 8.5, SLR = 1.8 m) the income loss is 104 €/ha higher in SC2, which represents a total amount of 2,184,000 €. Compared with the SC1 approach, SC2 showed reduced rice productivity but at the same time the sediment deficit was considerably lower, and consequently, the overall economic cost was lower.

Furthermore, the cost-benefit balance was most optimal when selecting the flushing as sediment extraction and transport technique.

The cost of applying the adaptation measure is considerably high but has a positive effect on the economic feasibility of rice farming. However, when making the cost-benefit balance, results show that the balance is mainly negative for all considered scenarios. The SC2 approach is more feasible to be applied, and in combination with the flushing technique, results in a less negative balance. Our economic analysis has some limitations, for instance, costs and benefits did not include the environmental ones, the price per kilogram of rice paid to farmers is expected to change in the future as well as the costs of sediment extraction and transport. We highlight that our economic analysis is simple and only pretends to qualitatively compare the costs and benefits of the different scenarios. In our study, we only have considered the economic income of rice production as a benefit but rice fields deliver more ecosystem services and hence benefits, like the prevention of salt intrusion through fresh water irrigation, and contribute to nutrient removal, biodiversity (*e.g.* vegetation, waterbirds, amphibians, fish), ecotourism, and fisheries (Natuhara, 2013; Ondiek et al., 2016). Wetlands are buffer zones against coastal flood risks, and a natural capital substitute for conventional flood protection investments such as dykes (Boyd and Banzhaf, 2007; Cheong et al., 2013; Temmerman et al., 2013). Moreover, wetlands work as a sediment trap and deltaic wetland sedimentation efficiently helps to compensate for SLR and subsidence (Temmerman and Kirwan, 2015; van der Deijl et al., 2017). The preservation of the Ebro Delta rice fields and wetlands is also perceived as important by local stakeholders for cultural, economic and ecological reasons. Moreover, the adaptation measure of recovering and adding fluvial sediments is supported by delta's inhabitants, including rice farmers (Ibáñez et al., 2014), which are –

in face of climate change and SLR – mainly concerned about the conservation of the delta's natural heritage (Romagosa and Pons, 2017), and the survival of rice cultivation.

The considered adaptation measure of "rising grounds" has other indirect benefits like the improvement of the maintenance of the reservoir capacity (Martín-Vide et al., 2004). Furthermore, the flushing of sediments during discharge pulse events will increase the turbidity in the river water, and as such can contribute to solve problems such as the reduction of the invasive zebra mussel population (Alcaraz et al., 2011), and the widespread aquatic macrophyte cover (Ibáñez et al., 2012), which has altered the river hydromorphology, leading to the phytoplankton collapse and black fly proliferation in the lower Ebro River. Nevertheless, there are also arguments against applying this adaptation measure. For example, flushing operations may negatively impact the hydropower companies and the irrigation system in the delta. Other costs related to flushing were not considered in this study such as the cost of cubic meter of fresh water in a future of water scarcity which could increase the competing demand for available freshwater. Therefore, all advantages and disadvantages (*i.e.* environmental costs and benefits in addition to the financial ones) need to be fully considered before applying this measure, and in this respect, our study is a first step in a series of further studies.

The proposed measure for sediment delivery to the delta is not fully a nature-based solution. Flushing partly relies on engineering and partly on natural transport of the sediments, with the river and the irrigation network (which is human made). Completely nature-based adaptation strategies are rarely applicable in strongly human-altered environments, such as the Ebro Delta, and hybrid approaches combining engineering and conservation or restoration of natural processes are often most feasible. Hybrid approaches have been applied for instance in the Mississippi Delta (Day et al., 2005), the Rhine Delta (Sigma Plan, 2011) and in densely populated coastal areas in New York after the Sandy storm (Pontee et al., 2016). As such, the options for adaptation to SLR that are evaluated in this study for the Ebro Delta, can be also considered as hybrid adaptation options, combining human interventions of sediment extraction from a reservoir, with (semi-)natural processes of sediment distribution through controlled river discharge pulses and through the network of irrigation channels in the delta.

5. Conclusions

Our study provides an assessment of the sediment volumes needed to sustain rice production and the Ebro Delta surface, thus including important ecological areas with rising sea level, and a first evaluation of the economic feasibility of introducing sediments, accumulated behind dams in the river catchment, back to the delta, through hybrid adaptation measures combining human interventions with a nature-based approach. The study contributes to increase the knowledge of the specific quantity of sediment required to maintain the Ebro Delta elevation under different scenarios of sea level rise over the 21st century. We developed a flood model to identify areas prone to be flooded and to be subject to decreased rice production, and calculated the sediment deficit needed to raise the land to compensate SLR. We developed a statistical relationship between organic matter and bulk density to obtain the sediment (volume and mass) deficit. Although with some limitations (*e.g.* environmental cost and benefits except the maintenance of rice production are not considered), we presented an approximate cost-benefit analysis comparing the cost of applying different techniques to extract and transport the sediment with the benefit of rice production. The proposed adaptation measure (*i.e.* sediment supply) showed a positive effect, minimizing the loss of rice production and economic income, being also beneficial for the maintenance of land elevation to face sea flooding, and can help to provide a better understanding of how the sediment supply will cope with a rising sea, being useful for rice farmers and for future sediment management plans.

Acknowledgments

Financial support was provided by European Union's Seventh Programme for Research, Technological Development and Demonstration under Grant Agreement No: FP7-ENV-2013-Two-Stage-603396-RISES-AM-. The authors would like to thank to Vegetal Protection Association (ADV) and local farmers for providing data, and to people from the Department of Ecosystem Management-ECOBE (University of Antwerp) for hosting Ana Genua-Olmedo during her research stay. We wish to thank Albert Rovira for his comments and suggestions. Ana Genua-Olmedo thanks to CESAM and to FCT/MCTES for the current financial support (UIDP/50017/2020+UIDB/50017/2020). Authors also acknowledge support from CERCA Programme (Generalitat de Catalunya).

References

Alcaraz, C., Caiola, N., Ibáñez, C., 2011. Bioaccumulation of pollutants in the zebra mussel from hazardous industrial waste and evaluation of spatial distribution using GAMs. Science of the Total Environment 409, 898–904. DOI: https://doi.org/10.1016/j.scitotenv.2010.11.015

Anthony, E.J., Brunier, G., Besset, M., Goichot, M., Dussouillez, P., Nguyen, V.L., 2015. Linking rapid erosion of the Mekong River delta to human activities. Scientific reports, 5, 1-12. DOI: https://doi.org/10.1038/srep14745

Anthony, E.J., Marriner, N., Morhange, C., 2014. Human influence and the changing geomorphology of Mediterranean deltas and coasts over the last 6000 years: from progradation to destruction phase? Earth-Science Reviews 139, 336–361. DOI: https://doi.org/10.1016/j.earscirev.2014.10.003

Auerbach, L.W., Goodbred, S.L., Mondal, D.R., Wilson, C.A., Ahmed, K.R., Roy, K., Steckler, M.S., Small, C., Gilligan, J.M., and Ackerly, B.A., 2015. Flood risk of natural and embanked landscapes on the Ganges-Brahmaputra tidal delta plain: Nature Climate Change 5, 153-157. DOI: https://doi.org/10.1038/nclimate2472

Bergillos, R.J., Ortega-Sánchez, M., 2017. Assessing and mitigating the landscape effects of river damming on the Guadalfeo River delta, southern Spain. Landscape and Urban Planning, 165, 117-129. DOI: http://dx.doi.org/10.1016/j.landurbplan.2017.05.002

Besset, M., Anthony, E.J., Bouchette, F., 2019. Multi-decadal variations in delta shorelines and their relationship to river sediment supply: An assessment and review. Earth-science reviews, 193, 199-219. DOI: https://doi.org/10.1016/j.earscirev.2019.04.018

Blazquez, C.A., Adams, T.M., Keillor, P., 2001. Optimization of mechanical dredging operations for sediment remediation. Journal of waterway, port, coastal, and ocean engineering, 127(6), 299-307. DOI: https://doi.org/10.1061/(ASCE)0733-950X(2001)127:6(299)

Bossard, M., Feranec, J., Otahel, J., 2000. CORINE land cover technical guide: Addendum 2000

Boyd, J., Banzhaf, S., 2007. What are ecosystem services? The need for standardized environmental accounting units. Ecological economics 63, 616–626. DOI: https://doi.org/10.1016/j.ecolecon.2007.01.002

Brockwell, P.J., Davis, R.A., 2002. Introduction to time series and forecasting. Springer Verlag, New York, p. 235.

Burnham, K.P., Anderson, D.R., 2002. Model selection and multimodel inference: a practical information-theoretic approach. Springer Verlag, New York, p. 274.

Cacchione, D.A., Drake, D.E., Losada, M.A., Medina, R., 1990. Bottom-boundary-layer measurements on the continental shelf off the Ebro River, Spain. Marine Geology 95, 179–192. DOI: https://doi.org/10.1016/0025-3227(90)90115-Z

Calvo-Cubero, J., Ibánez, C., Rovira, A., Sharpe, P.J., Reyes, E., 2013. Mineral versus organic contribution to vertical accretion and elevation change in restored marshes (Ebro Delta, Spain). Ecological Engineering 61, 12–22. DOI: https://doi.org/10.1016/j.ecoleng.2013.09.047

Chapman, A., Darby, S., 2016. Evaluating sustainable adaptation strategies for vulnerable mega-deltas using system dynamics modelling: Rice agriculture in the Mekong Delta's An Giang Province, Vietnam. Science of the Total Environment 559, 326–338. DOI: https://doi.org/10.1016/j.scitotenv.2016.02.162

Cheong, S.-M., Silliman, B., Wong, P.P., Van Wesenbeeck, B., Kim, C.-K., Guannel, G., 2013. Coastal adaptation with ecological engineering. Nature Climate Change 3, 787. DOI: https://doi.org/10.1038/nclimate1854

Church, J.A., Clark, P.U., Cazenave, A., Gregory, J.M., Jevrejeva, S., Levermann, A., Merrifield, M. a., Milne, G. a., Nerem, R.., Nunn, P.D., Payne, A.J., Pfeffer, W.T., Stammer, D., Unnikrishnan, A.S., 2013. Sea level change. Climate Change. 2013. The Physical Science Basis. Contribution of Working Group I to the Fifth Assessment Report of the Intergovernmental Panel on Climate Change [Stocker, T.F., D. Qin, G.-K. Plattner, M. Tignor, S.K. Allen, J. Boschung, A. Nauels, Y. Xia,

V. Bex and P.M. Midgley (eds.)]. Cambridge University Press, Cambridge, United Kingdom and New York, NY, USA.

Curtis, R.O., Post, B.W., 1964. Estimating bulk density from organic-matter content in some Vermont forest soils. Soil Science Society of America Journal 28, 285–286. DOI: https://doi.org/10.2136/sssaj1964.03615995002800020044x

Darby, S.E., Nicholls, R.J., Rahman, M.M., Brown, S., Karim, R., 2018. A sustainable future supply of fluvial sediment for the Ganges-Brahmaputra Delta. Ecosystem Services for Well-Being in Deltas, 277-291. DOI: https://doi.org/10.1007/978-3-319-71093-8_15

Day, J.W., Arancibia, A.Y., Mitsch, W.J., Lara-Dominguez, A.L., Day, J.W.J.N., Ko, J.-Y., Lane, R., Lindsey, J., Lomeli, D.Z., 2003. Using ecotechnology to address water quality and wetland habitat loss problems in the Mississippi basin: a hierarchical approach. Biotechnoly Advances 22, 135–159. DOI: https://doi.org/10.1016/j.biotechadv.2003.08.012

Day, J.W., Barras, J., Clairain, E., Johnston, J., Justic, D., Kemp, G.P., Ko, J.-Y., Lane, R., Mitsch, W.J., Steyer, G., Templet, P., Yañez-Arancibia, A., 2005. Implications of global climatic change and energy cost and availability for the restoration of the Mississippi delta. Ecological engineering 24, 253–265. DOI: https://doi.org/10.1016/j.ecoleng.2004.11.015

Day, J.W., Boesch, D.F., Clairain, E.J., Kemp, G.P., Laska, S.B., Mitsch, W. J., Orth, K., Mashriqui, H., Reed, D.J., Shabman, L., Simenstad, C.A., Streever, B.J., Twilley, R. R., Watson, C.C., Wells, J.T., and Whigham, D.F., 2007. Restoration of the Mississippi Delta: lessons from hurricanes Katrina and Rita: Science, 315(5819), 1679-1684. DOI: https://doi.org/10.1126/science.1137030

Day, J.W., Lane, R.R., D'Elia, C.F., Wiegman, A.R., Rutherford, J.S., Shaffer, G.P., Brantley, C.G., Kemp, G.P., 2018. Large infrequently operated river diversions for Mississippi delta restoration. In: Day J., Erdman J. (eds) Mississippi Delta Restoration (pp. 113-133). Estuaries of the World. Springer, Cham. DOI: https://doi.org/10.1007/978-3-319-65663-2_8

Ericson, J.P., Vörösmarty, C.J., Dingman, S.L., Ward, L.G., Meybeck, M., 2006. Effective sea-level rise and deltas: causes of change and human dimension implications. Global and Planetary Change, 50(1-2), 63-82. DOI: https://doi.org/10.1016/j.gloplacha.2005.07.004

Fatorić, S., Chelleri, L., 2012. Vulnerability to the effects of climate change and adaptation: the case of the Spanish Ebro Delta. Ocean & Coastal Management 60, 1–10. DOI: https://doi.org/10.1016/j.ocecoaman.2011.12.015

Gedan, K.B., Kirwan, M.L., Wolanski, E., Barbier, E.B., Silliman, B.R., 2011. The present and future role of coastal wetland vegetation in protecting shorelines: answering recent challenges to the paradigm. Climatic Change 106, 7–29. DOI: https://doi.org/10.1007/s10584-010-0003-7

Genua-Olmedo, A., Alcaraz, C., Caiola, N., Ibáñez, C., 2016. Sea level rise impacts on rice production: The Ebro Delta as an example. Science of the Total Environment 571, 1200-1210. DOI: https://doi.org/10.1016/j.scitotenv.2016.07.136

Giosan, L., Syvitski, J., Constantinescu, S., Day, J., 2014. Climate change: protect the world's deltas. Nature News, 516 31-33. DOI: https://doi.org/10.1038/516031a

Harvey, B.C., Lisle, T.E., 1998. Effects of suction dredging on streams: a review and an evaluation strategy. Fisheries, 23(8), 8-17. DOI: https://doi.org/10.1577/1548-8446(1998)023<0008:EOSDOS>2.0.CO;2

HaskoningDHV, R., Wageningen, U.R., Deltares, R., 2013. Mekong Delta Plan: Long-Term Vision and Strategy for a Safe, Prosperous and Sustainable Delta. Prepared under the Strategic Partnership Arrangement on Climate Change Adaptation and Water Management between the Netherlands and Vietnam. Hanoi and Amersfoort. Link: https://www.deltares.nl/app/uploads/2014/01/Mekong-delta-plan-Long-term-vision-and-strategy.pdf

Ibáñez, C., Caiola, N., Rovira, A., Real, M., 2012. Monitoring the effects of floods on submerged macrophytes in a large river. Science of the Total Environment 440, 132–139. https://doi.org/10.1016/j.scitotenv.2012.07.073

Ibáñez, C., Canicio, A., Day, J.W., Curcó, A., 1997. Morphologic development, relative sea level rise and sustainable management of water and sediment in the Ebre Delta, Spain. Journal of Coastal Conservation 3, 191–202. DOI: https://doi.org/10.1007/BF02908194

Ibáñez, C., Day, J.W., Reyes, E., 2014. The response of deltas to sea-level rise: natural mechanisms and management options to adapt to high-end scenarios. Ecological engineering 65, 122–130. DOI: https://doi.org/10.1016/j.ecoleng.2013.08.002

Jansson, M.B., Erlingsson, U., 2000. Measurement and quantification of a sedimentation budget for a reservoir with regular flushing. Regulated Rivers: Research & Management: An International Journal Devoted to River Research and Management, 16, 279–306. DOI: https://doi.org/10.1002/(SICI)1099-1646(200005/06)16:3<279::AID-RRR586>3.0.CO;2-S

Jevrejeva, S., Grinsted, A., Moore, J.C., 2014. Upper limit for sea level projections by 2100 Environmental Research Letters 9, 104008. DOI: https://doi.org/10.1088/1748-9326/9/10/104008

Ji, U., Julien, P.Y., Park, S.K., 2011. Sediment flushing at the Nakdong river estuary barrage. Journal of Hydraulic Engineering, 137, 1522-1535. DOI: https://doi.org/10.1061/(ASCE)HY.1943-7900.0000395

Jiménez, J.A., Sánchez-Arcilla, A., 1993. Medium-term coastal response at the Ebro delta, Spain. Marine Geology 114, 105–118. DOI: https://doi.org/10.1016/0025-3227(93)90042-T

Kemp, G.P., Day, J.W., Rogers, J.D., Giosan, L., Peyronnin, N., 2016. Enhancing mud supply from the Lower Missouri River to the Mississippi River Delta USA: Dam bypassing and coastal restoration. Estuarine, Coastal and Shelf Science, 183, 304-313. DOI: http://dx.doi.org/10.1016/j.ecss.2016.07.008

Kirwan, M.L., Megonigal, J.P., 2013. Tidal wetland stability in the face of human impacts and sea-level rise. Nature 504, 53–60. DOI: https://doi.org/10.1038/nature12856

Kirwan, M.L., Temmerman, S., Skeehan, E.E., Guntenspergen, G.R., Fagherazzi, S., 2016. Overestimation of marsh vulnerability to sea level rise. Nature Climate Change 6, 253. DOI: https://doi.org/10.1038/nclimate2909

Kondolf, G.M., Gao, Y., Annandale, G.W., Morris, G.L., Jiang, E., Zhang, J., Cao, Y., Carling, P., Fu, K., Guo, Q., Hotchkiss, R., Peteuil, C., Sumi, T., Wang, H-W., Wang, Z., Wei, Z., Wu, B., Wu, C., Yang, C.T., 2014. Sustainable sediment management in reservoirs and regulated rivers: Experiences from five continents. Earth's Future, 2(5), 256-280. DOI: https://doi.org/10.1002/2013EF000184

López-Dóriga, U., Jiménez, J.A., 2020. Impact of Relative Sea-Level Rise on Low-Lying Coastal Areas of Catalonia, NW Mediterranean, Spain. Water, 12(11), 3252. DOI: https://doi.org/10.3390/w12113252

Maggini, R., Lehmann, A., Zimmermann, N.E., Guisan, A., 2006. Improving generalized regression analysis for the spatial prediction of forest communities. Journal of Biogeography 33, 1729–1749. DOI: https://doi.org/10.1111/j.1365-2699.2006.01465.x

MAGRAMA, 2017. Anuario de estadística agraria, Madrid (accessed: 24.04.2017). URL: http://www.magrama.gob.es/

Martín-Vide, J.P., Mazza de Almeida, G.A., Helmbrecht, J., Ferrer, C., Rojas Lara, D.L., 2004. Estudio técnico-económico de alternativas del programa para corregir la subsidencia y regresión del delta del Ebro. Universitat Politècnica de Catalunya. Technical Report for Fundación Nueva Cultura del Agua y la Agència Catalana de l'Aigua.

McGranahan, G., Balk, D., Anderson, B., 2007. The rising tide: assessing the risks of climate change and human settlements in low elevation coastal zones. Environment and Urbanization 19, 17–37. DOI: https://doi.org/10.1177/0956247807076960

Natuhara, Y., 2013. Ecosystem services by paddy fields as substitutes of natural wetlands in Japan. Ecological Engineering 56, 97–106. DOI: https://doi.org/10.1016/j.ecoleng.2012.04.026

Nicholls, R.J., Cazenave, A., 2010. Sea-level rise and its impact on coastal zones. Science 328, 1517–1520. DOI: https://doi.org/10.1126/science.1185782

Nicholls, R.J., Wong, P.P., Burkett, V., Codignotto, J., Hay, J., McLean, R., Ragoonaden, S., Woodroffe, C.D., Abuodha, P.A.O., Arblaster, J., 2007. Coastal systems and low-lying areas. Climate Change 2007: Impacts, Adaptation and Vulnerability. Contribution of Working Group II to the Fourth Assessment Report of the Intergovernmental Panel on Climate Change, Eds., Cambridge University Press, Cambridge, UK, 315-356.

Ondiek, R.A., Kitaka, N., Oduor, S.O., 2016. Assessment of provisioning and cultural ecosystem services in natural wetlands and rice fields in Kano floodplain, Kenya. Ecosystem services, 21, 166-173. DOI: https://doi.org/10.1016/j.ecoser.2016.08.008

Périé, C., Ouimet, R., 2008. Organic carbon, organic matter and bulk density relationships in boreal forest soils. Canandian Journal of Soil Science 88, 315–325. DOI: https://doi.org/10.4141/CJSS06008

Peyronnin, N., Green, M., Richards, C.P., Owens, A., Reed, D., Chamberlain, J., Groves, D.G., Rhinehart, W.K., Belhadjali, K., 2013. Louisiana's 2012 coastal master plan: overview of a science-based and publicly informed decision-making process. Journal of Coastal Research 67, 1–15. DOI: https://doi.org/10.2112/SI_67_1.1

Pont, D., Day, J.W., Hensel, P., Franquet, E., Torre, F., Rioual, P., Ibànez, C., Coulet, E., 2002. Response scenarios for the deltaic plain of the Rhone in the face of an acceleration in the rate of sea-level rise with special attention to Salicornia-type environments. Estuaries and Coasts 25, 337–358. DOI: https://doi.org/10.1007/BF02695978

Pontee, N., Narayan, S., Beck, M.W., Hosking, A.H., 2016. Nature-based solutions: lessons from around the world. In Proceedings of the Institution of Civil Engineers-Maritime Engineering (Vol. 169, No. 1, pp. 29-36). Thomas Telford Ltd. DOI: https://doi.org/10.1680/jmaen.15.00027

Roca, M., Martín-Vide, J.P., 2005. Arrastre controlado de sedimento en el embalse de Riba-Roja d'Ebre. Universitat Politècnica de Catalunya. Technical Report for United Research Services España S.L. (URS).

Rogers, K.G., Syvitski, J.P.M., Overeem, I., Higgins, S., Gilligan, J.M., 2013. Farming practices and anthropogenic delta dynamics. Deltas: Landforms, Ecosystems and Human Activities, Redbook Proceedings of HP1, IAHS Publ 358, 133–142.

Romagosa, F., Pons, J., 2017. Exploring local stakeholders' perceptions of vulnerability and adaptation to climate change in the Ebro delta. Journal of Coastal Conservation 21, 223–232. https://doi.org/10.1007/s11852-017-0493-9

Rovira, A., Ibáñez, C., 2007. Sediment management options for the lower Ebro River and its delta. Journal of Soils & Sediments 7, 285–295. DOI: https://doi.org/10.1065/jss2007.08.244

Rovira, A., Ibáñez, C., 2015. Restoring sediment fluxes downstream of large dams: The case of the lower Ebro River. Basins under Pressure: Ebro basin, 5.

Sánchez-Arcilla, A., Jiménez, J.A., Valdemoro, H.I., Gracia, V., 2008. Implications of climatic change on Spanish Mediterranean low-lying coasts: The Ebro delta case. Journal of Coastal Research, 242, 306–316. DOI: https://doi.org/10.2112/07A-0005.1

Schuerch, M., Spencer, T., Temmerman, S., Kirwan, M.L., Wolff, C., Lincke, D., McOwen, C.J., Pickering, M.D., Reef, R., Vafeidis, A.T., Hinkel, J., Nicholls, R.J., and Brown, S., 2018. Future response of global coastal wetlands to sea-level rise: Nature, v. 56, p. 231-234. DOI: https://doi.org/10.1038/s41586-018-0476-5

Sigma Plan, 2011. Sigma Plan: http://www.sigmaplan.be/en

Syvitski, J., Kettner, A.J., Overeem, I., Hutton, E.W., Hannon, M.T., Brakenridge, G.R., Day, J., Vörösmarty, C., Saito, Y., Giosan, L., Nicholls, R.J., 2009. Sinking deltas due to human activities. Nature Geoscience, 2, 681-686. DOI:

https://doi.org/10.1038/ngeo629

Temmerman, S., Kirwan, M.L., 2015. Building land with a rising sea. Science 349, 588–589. DOI: https://doi.org/10.1126/science.aac8312

Temmerman, S., Meire, P., Bouma, T.J., Herman, P.M.J., Ysebaert, T., De Vriend, H.J., 2013. Ecosystem-based coastal defence in the face of global change. Nature 504, 79-83. DOI: https://doi.org/10.1038/nature12859

Tessler, Z.D., Vörösmarty, C.J., Grossberg, M., Gladkova, I., Aizenman, H., Syvitski, J.P.M., Foufoula-Georgiou, E., 2015. Profiling risk and sustainability in coastal deltas of the world. Science 349, 638–643. DOI: https://doi.org/10.1126/science.aab3574

Turner, R.E., Streever, B., 2002. Approaches to coastal wetland restoration: Northern Gulf of Mexico. SPB Academic Publishing, Hague, The Netherlands, 147 pp

van der Deijl, E.C., van der Perk, M., Middelkoop, H., 2017. Factors controlling sediment trapping in two freshwater tidal wetlands in the Biesbosch area, The Netherlands. Journal of Soils and Sediments 1–17. DOI: https://doi.org/10.1007/s11368-017-1729-x

Van Vuuren, D.P., Edmonds, J., Kainuma, M., Riahi, K., Thomson, A., Hibbard, K., Hurtt, G.C., Kram, T., Krey, V., Lamarque, J.-F., 2011. The representative concentration pathways: an overview. Climatic Change 109, 5. DOI: https://doi.org/10.1007/s10584-011-0148-z

Wang, Z., Chunhong, H.U., 2009. Strategies for managing reservoir sedimentation. International Journal of Sediment Research 24, 369–384. DOI: https://doi.org/10.1016/S1001-6279(10)60011-X

Warren, R.S., Niering, W.A., 1993. Vegetation Change on a Northeast Tidal Marsh: Interaction of Sea-Level Rise and Marsh Accretion. Ecology 74, 96–103. DOI: https://doi.org/10.2307/1939504

Whittingham, M.J., Swetnam, R.D., Wilson, J.D., Chamberlain, D.E., Freckleton, R.P., 2005. Habitat selection by yellowhammers Emberiza citrinella on lowland farmland at two spatial scales: implications for conservation management. Journal of Applied Ecology 42, 270–280. DOI: https://doi.org/10.1111/j.1365-2664.2005.01007.x

Wohl, E.E., Cenderelli, D.A., 2000. Sediment deposition and transport patterns following a reservoir sediment release. Water Resources Research 36, 319–333. DOI: https://doi.org/10.1029/1999WR900272

Woodroffe, C.D., Nicholls, R.J., Saito, Y., Chen, Z., Goodbred, S.L., 2006. Landscape variability and the response of Asian megadeltas to environmental change. In Global change and integrated coastal management (pp. 277-314). Springer, Dordrecht.

Figure 1. Location of the Ebro Delta (**a**); the Digital Elevation Model (DEM, m relative to mean sea level) (**b**); distribution of the rice fields along with organic matter sampling points (**c**); irrigation channels network (**d**); and habitats distribution (**e**).

Figure 2. Relationship between predicted and observed values of soil bulk density (BD) (**a**), and soil organic matter content (OM) (**b**). Data were log-transformed and refer to the calibration process.

Figure 3. Simulation of the Ebro Delta flooding under mean RCP 4.5 and upper limit RCP 8.5 SLR scenarios (**a**). See Supplementary Figure 1 for complementary information. Flooded area of rice fields and Ebro Delta under SLR scenarios (**b**). See Supplementary Table 4 for complementary information.

Figure 4. Spatial distribution of surface elevation (m relative to mean sea level), sediment volume deficit (m^3/m^2), sediment mass deficit (kg/m^2), soil salinity (dS/m) and rice production index (%) under the mean RCP 4.5 and upper limit RCP 8.5 SLR scenarios in 2100 for SC1 and SC2. SC1, considers the total sediment volume deficit needed to maintain deltaic surface elevation relative to mean sea level as in the reference state (*i.e.* 2010), and SC2 considers the total sediment volume deficit needed to raise inundated areas just enough to compensate the RCP SLR scenario. See Supplementary Table 4 for complementary information.

Figure 5. Evolution of sediment volume deficit and equivalent mass during the 21st century for the considered SLR scenarios, and for SC1 and SC2 in rice fields (210 km^2) and in the other deltaic areas (80 km^2). SC1 considers the total sediment volume deficit needed to maintain deltaic surface elevation relative to mean sea level as in the reference state (*i.e.* 2010), and SC2 considers the total sediment volume deficit needed to raise

inundated areas just enough to compensate the RCP SLR scenario. See Supplementary Table 4 for complementary information.

Figure 6. Evolution of mean value of soil salinity (**a**), rice production index (**b**), and income (**c**) during the 21st century for the considered SLR scenarios for SC2. SC1 is not shown because remains constant over time as in the reference state (mean soil salinity = 5.53 dS/m; mean rice production = 61.2 %; mean income = 2,359.38 €/ha). See Supplementary Table 4 for complementary information.

Figure 7. Estimated cost of the sediment extraction and transport by pipeline for mechanical dredging, suction dredging and flushing techniques. The cost is the average of the minimum and maximum cost (see Table 1 and Supplementary Table 5) under the simulated SLR scenarios. SC1 considers the total sediment volume deficit needed to maintain deltaic surface elevation relative to mean sea level as in the reference state (*i.e.* 2010), and SC2 considers the total sediment volume deficit needed to raise inundated areas just enough to compensate the RCP SLR scenario.

Table 1. Cost of sediment extraction and transport (in €/m^3) from Riba-Roja reservoir to the start of the irrigation network in Xerta. The cost of extraction varied on the water depth. The cost of the extra transport only considers the pipeline. The total cost is the sum of the cost of extraction and extra transport at different water depths. Table modified from Roca and Martín-Vide (2005).

	Total cost of extraction			**Total cost**	
Engineering technique	**Water depth** < 5 m	**Water depth** > 5 m	**Extra transport**	**Min**	**Max**
Mechanical dredging	7.2	8.3	1.4	8.6	9.7
Suction dredging	3.1	13	1.4	4.5	14.4
Flusing flood	0.54*		0	0.54	0.54

* The cost attributed is the price for an energy consumer of the loss of production that the hydroelectric company would have due to the emptiness of the reservoir. There is not transport cost for flushing.

Table 2. Results from the information-theoretic framework analysis to predict organic matter content in the Ebro Delta. Model regression coefficients (*β*) are shown, bias is the difference between the AICc selected model and the full model coefficients. Model variables were log-transformed prior to the analysis. See Supplementary Table 2 for a detailed list of variables initially included.

Model parameters	***β***	**Bias**
Intercept	-0.610	-0.473
Euclidean Distance to the inner border (m)	-0.009	-0.029
Euclidean Distance to the mouth (m)	0.031	0.035
Surface elevation (m)	-0.010	3.753
Quadratic soil salinity (dS/m)	0.032	0.127
Quadratic Euclidean distance to the coast	0.005	-0.017
Quadratic surface elevation (m)	-0.148	-2.863

Figure 1

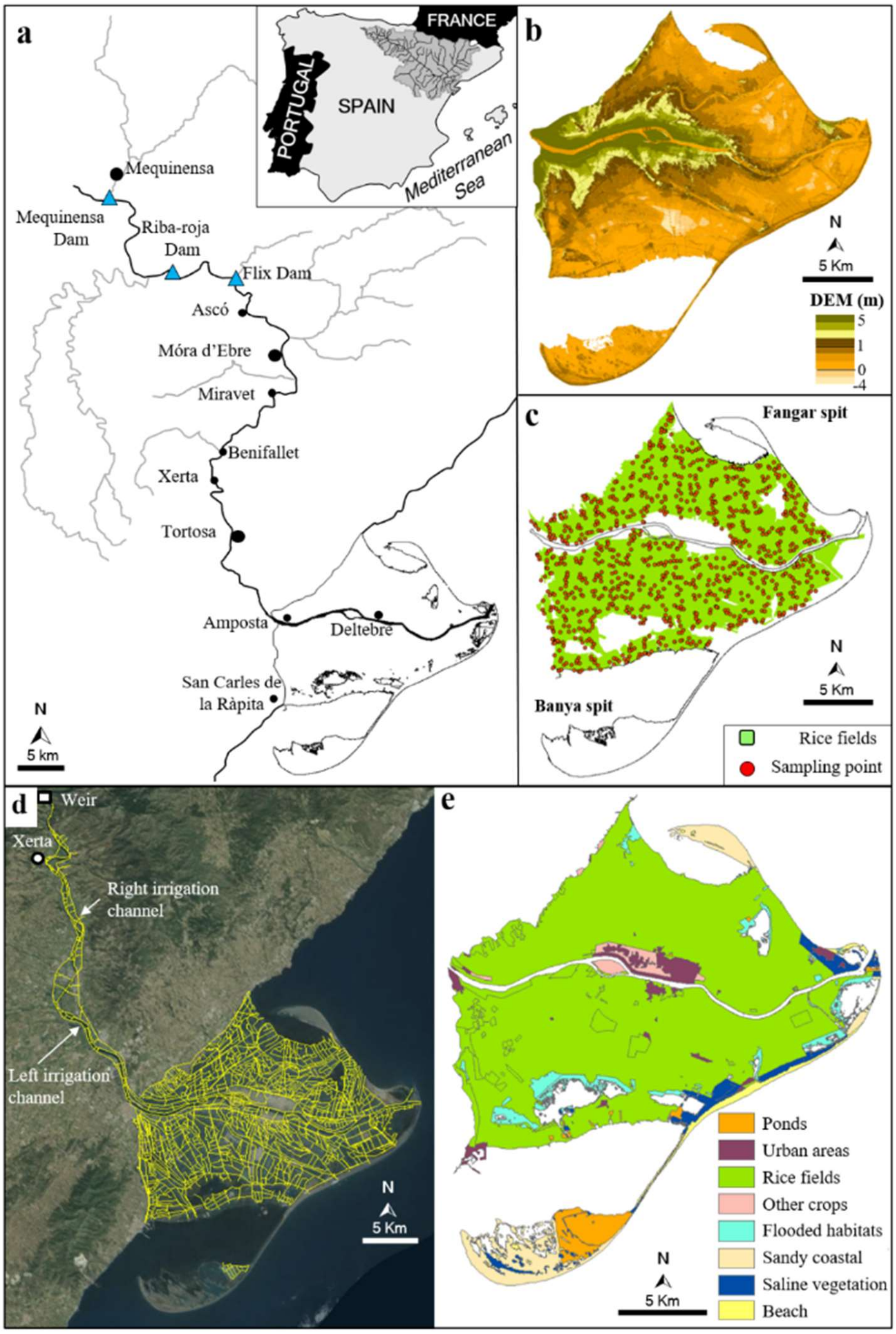
a
FRANCE
PORTUGAL
SPAIN
Mediterranean Sea
Mequinensa
Mequinensa Dam
Riba-roja Dam
Flix Dam
Ascó
Móra d'Ebre
Miravet
Benifallet
Xerta
Tortosa
Amposta
Deltebre
San Carles de la Ràpita
N
5 km
b
N
5 Km
DEM (m)
5
1
0
-4
c
Fangar spit
Banya spit
N
5 Km
Rice fields
Sampling point
d
Weir
Xerta
Right irrigation channel
Left irrigation channel
N
5 Km
e
Ponds
Urban areas
Rice fields
Other crops
Flooded habitats
Sandy coastal
Saline vegetation
Beach
N
5 Km

Figure 2

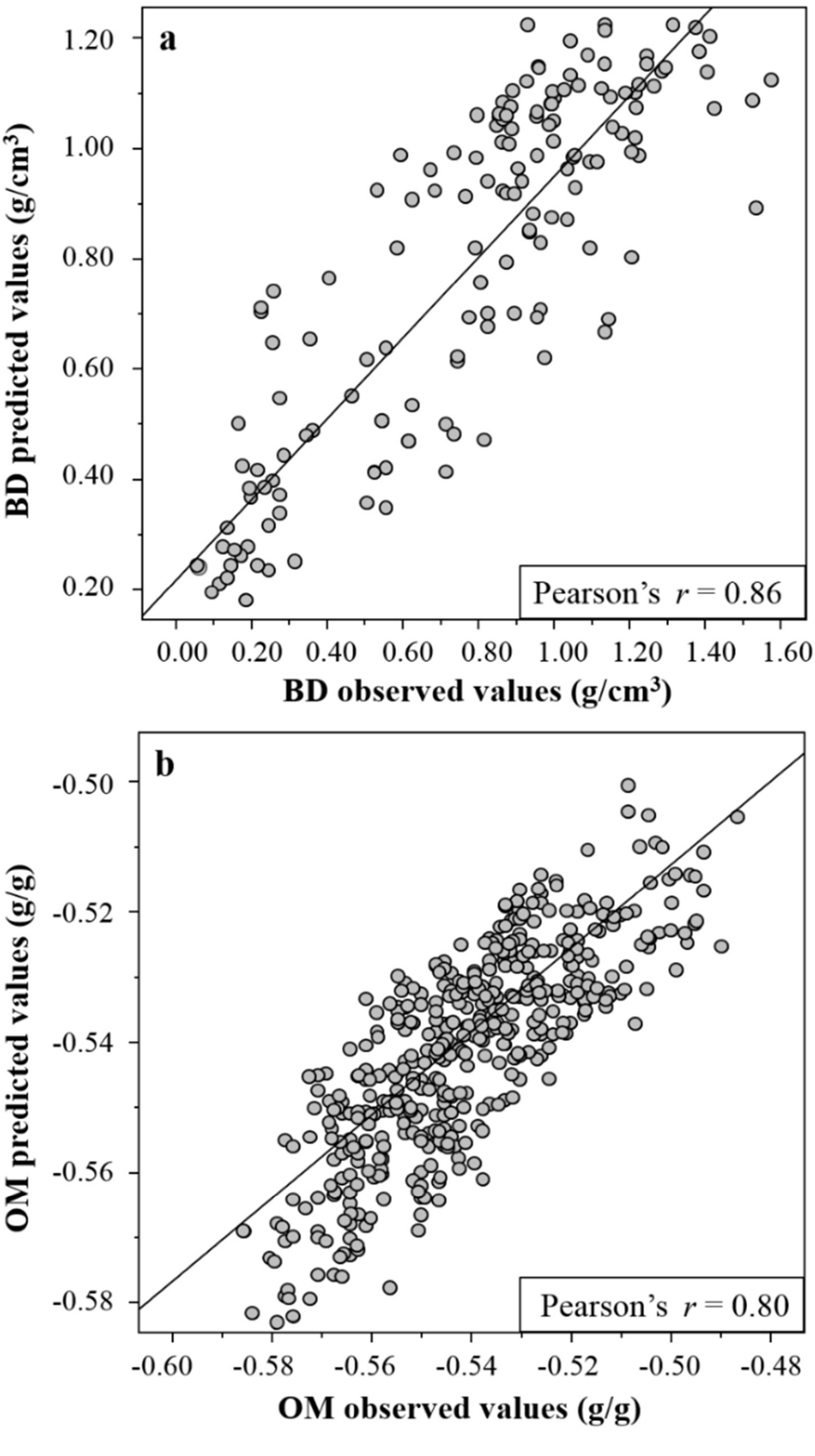
a
1.20
1.00
0.80
0.60
0.40
0.20
BD predicted values (g/cm³)
0.00 0.20 0.40 0.60 0.80 1.00 1.20 1.40 1.60
BD observed values (g/cm³)
Pearson's r = 0.86
b
-0.50
-0.52
-0.54
-0.56
-0.58
OM predicted values (g/g)
-0.60 -0.58 -0.56 -0.54 -0.52 -0.50 -0.48
OM observed values (g/g)
Pearson's r = 0.80

Figure 3

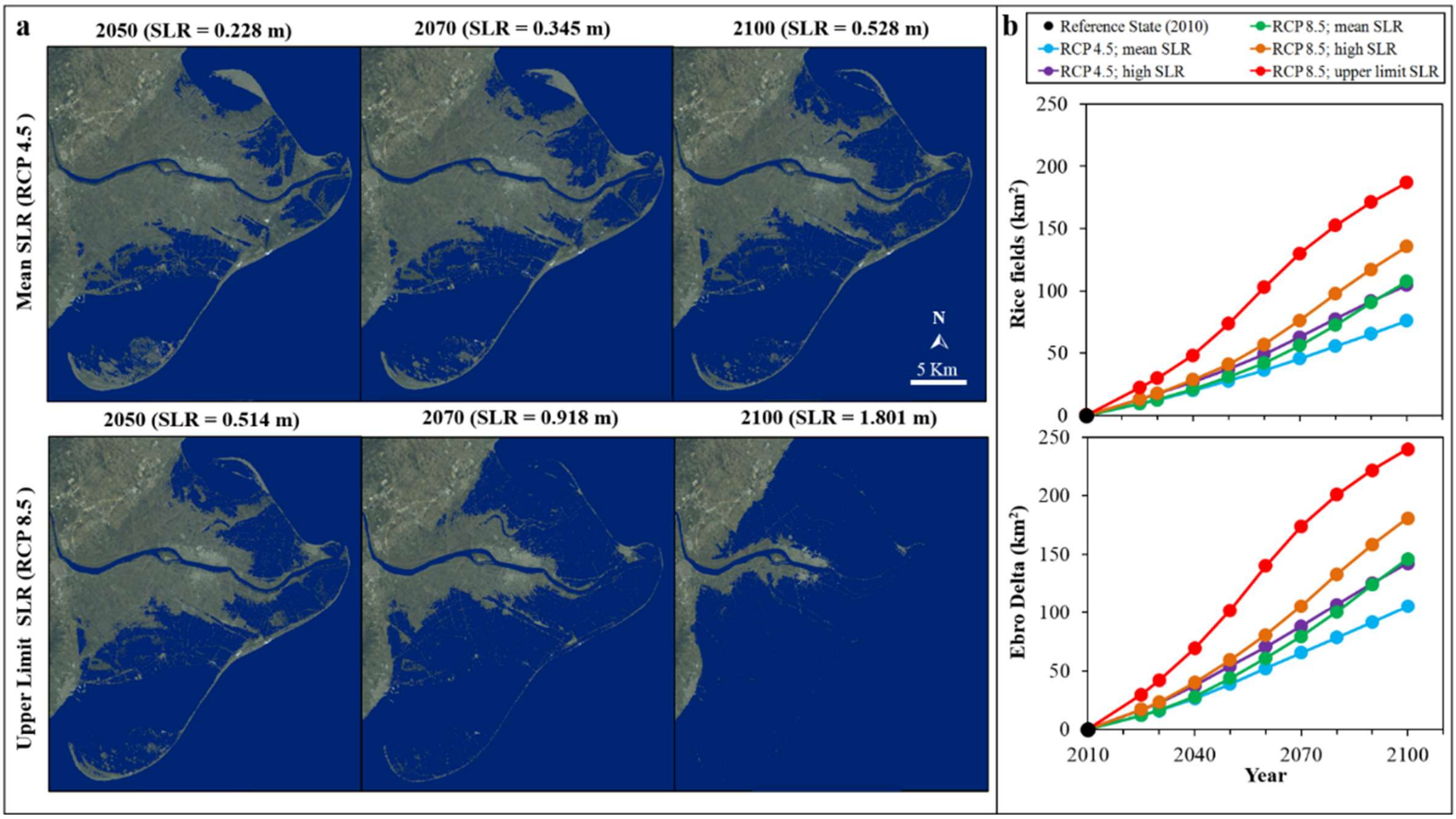
a
2050 (SLR = 0.228 m)
2070 (SLR = 0.345 m)
2100 (SLR = 0.528 m)
Mean SLR (RCP 4.5)
N
5 Km
2050 (SLR = 0.514 m)
2070 (SLR = 0.918 m)
2100 (SLR = 1.801 m)
Upper Limit SLR (RCP 8.5)
b
Reference State (2010)
RCP 4.5; mean SLR
RCP 4.5; high SLR
RCP 8.5; mean SLR
RCP 8.5; high SLR
RCP 8.5; upper limit SLR
Rice fields (km²)
Ebro Delta (km²)
0
50
100
150
200
250
2010
2040
2070
2100
Year

Figure 4

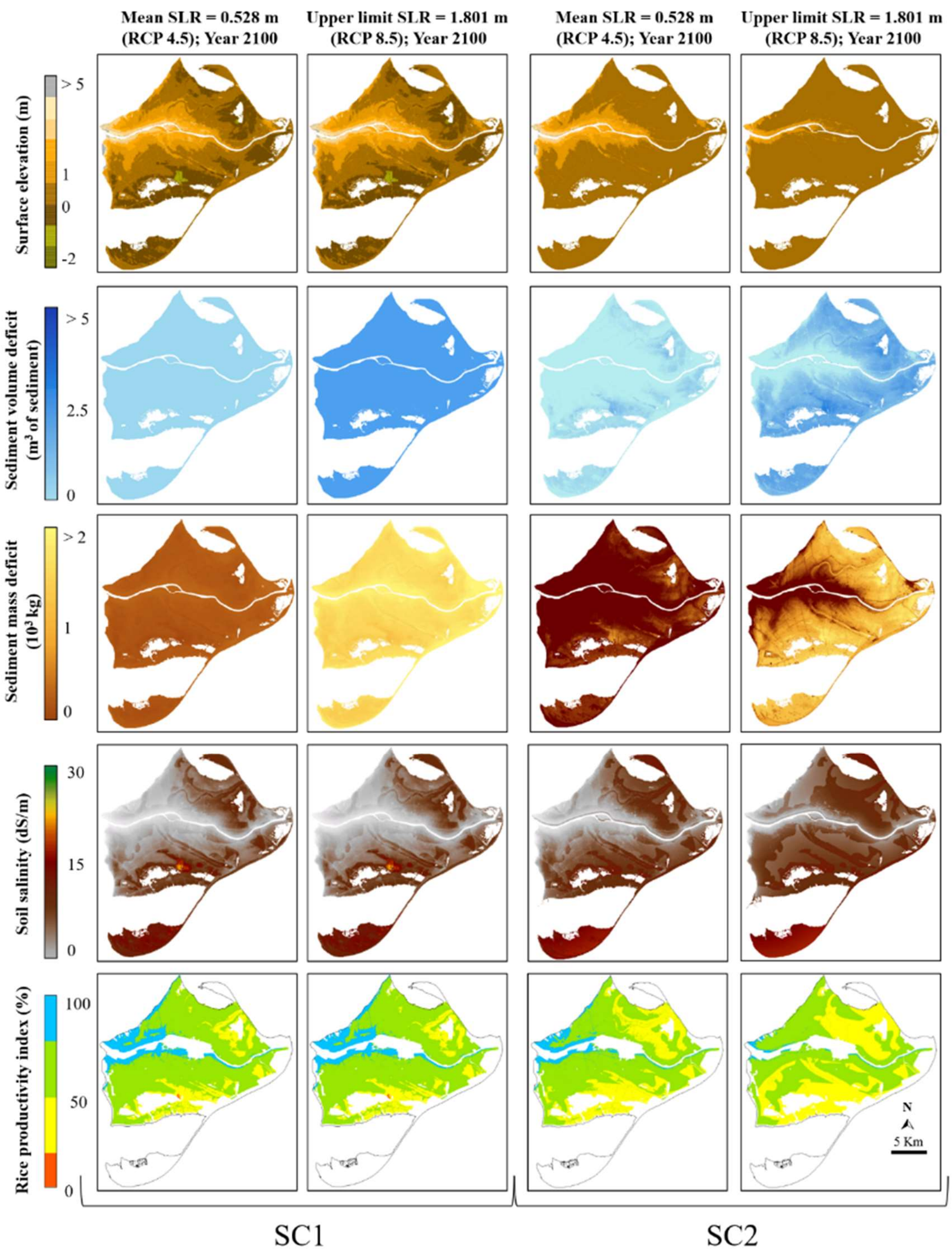

Mean SLR = 0.528 m (RCP 4.5); Year 2100
Upper limit SLR = 1.801 m (RCP 8.5); Year 2100
Mean SLR = 0.528 m (RCP 4.5); Year 2100
Upper limit SLR = 1.801 m (RCP 8.5); Year 2100
Surface elevation (m)
> 5
1
0
-2
Sediment volume deficit (m³ of sediment)
> 5
2.5
0
Sediment mass deficit (10³ kg)
> 2
1
0
Soil salinity (dS/m)
30
15
0
Rice productivity index (%)
100
50
0
N
5 Km
SC1
SC2

Figure 5

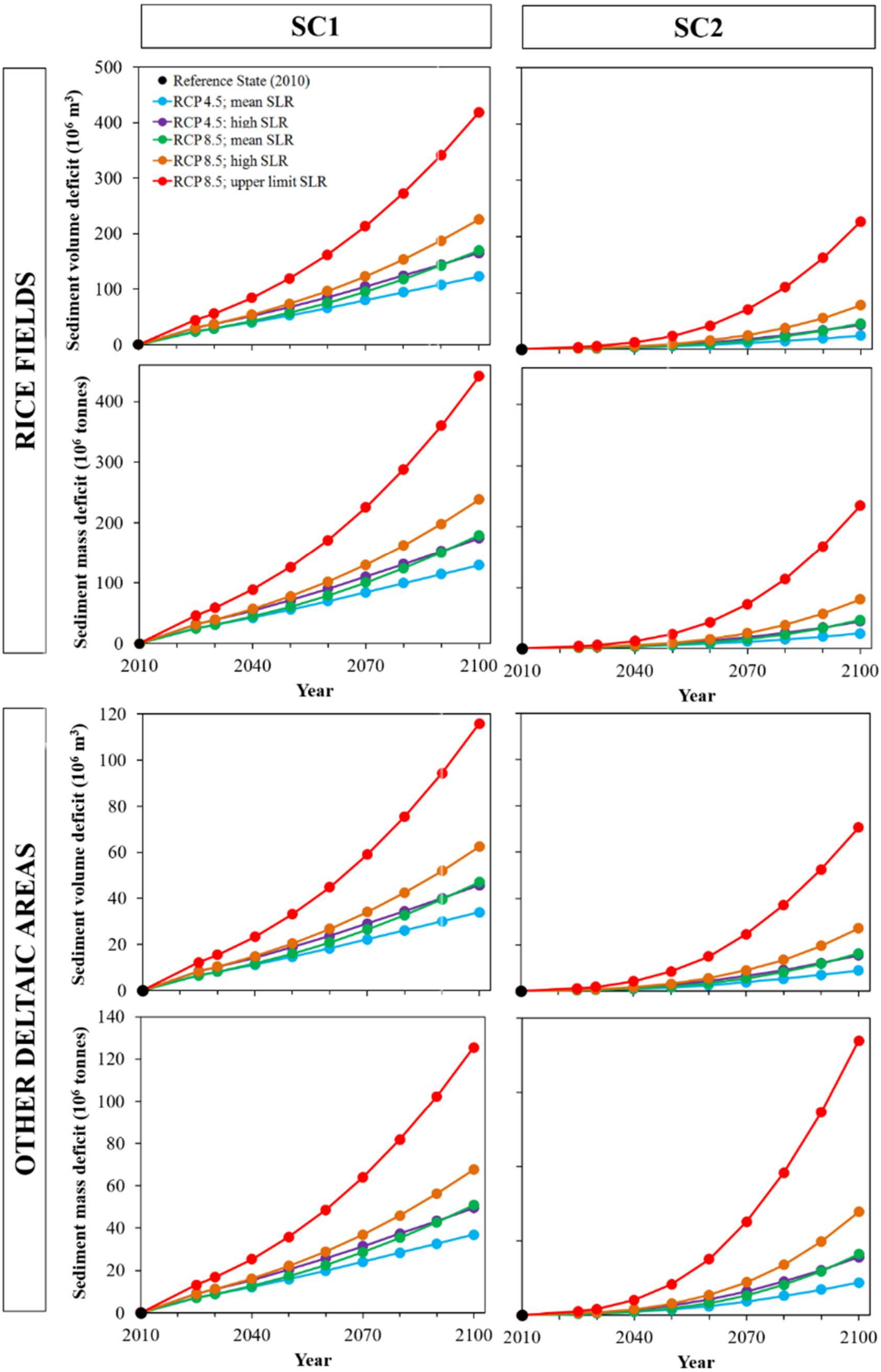

SC1
SC2
RICE FIELDS
OTHER DELTAIC AREAS
Reference State (2010)
RCP4.5; mean SLR
RCP4.5; high SLR
RCP8.5; mean SLR
RCP8.5; high SLR
RCP8.5; upper limit SLR
Sediment volume deficit (10⁶ m³)
Sediment mass deficit (10⁶ tonnes)
Year
2010
2040
2070
2100

Figure 6

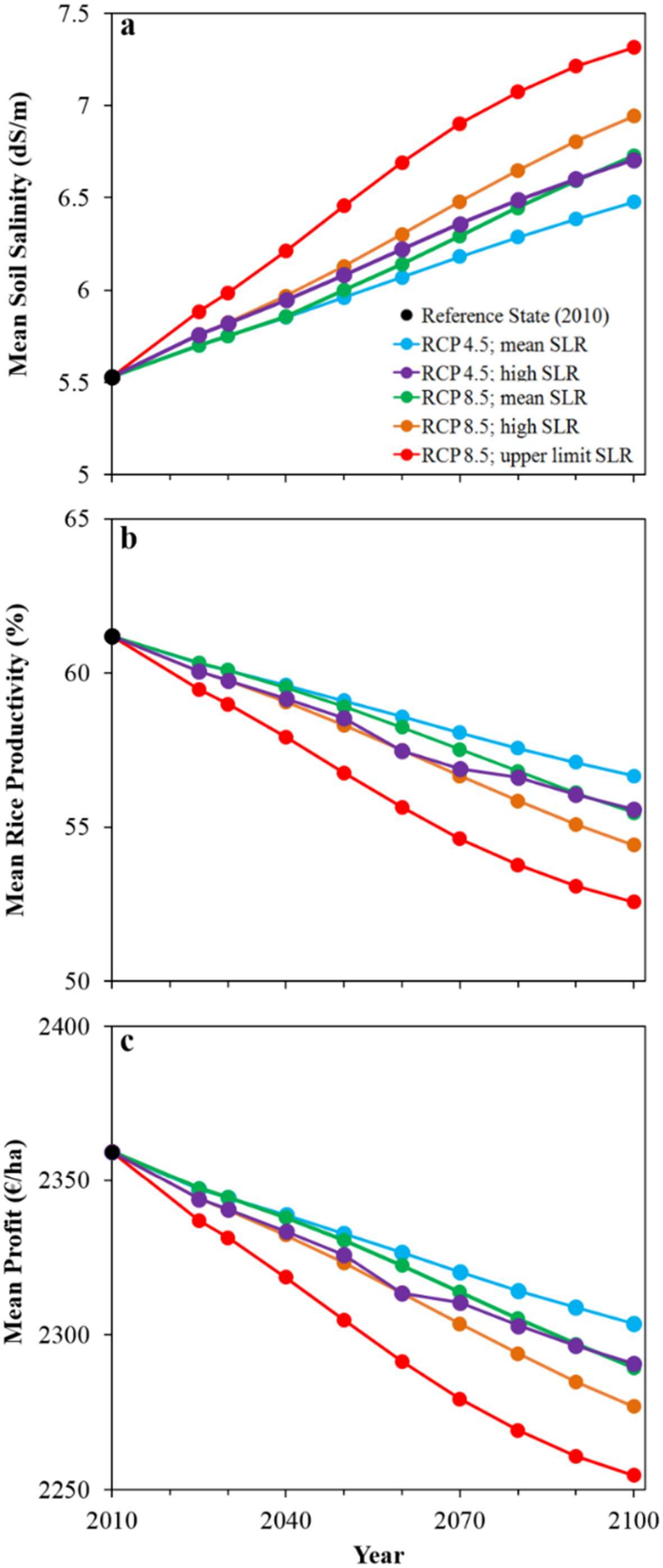
a
b
c
Mean Soil Salinity (dS/m)
Mean Rice Productivity (%)
Mean Profit (€/ha)
Year
Reference State (2010)
RCP 4.5; mean SLR
RCP 4.5; high SLR
RCP 8.5; mean SLR
RCP 8.5; high SLR
RCP 8.5; upper limit SLR
7.5
7
6.5
6
5.5
5
65
60
55
50
2400
2350
2300
2250
2010
2040
2070
2100

Figure 7

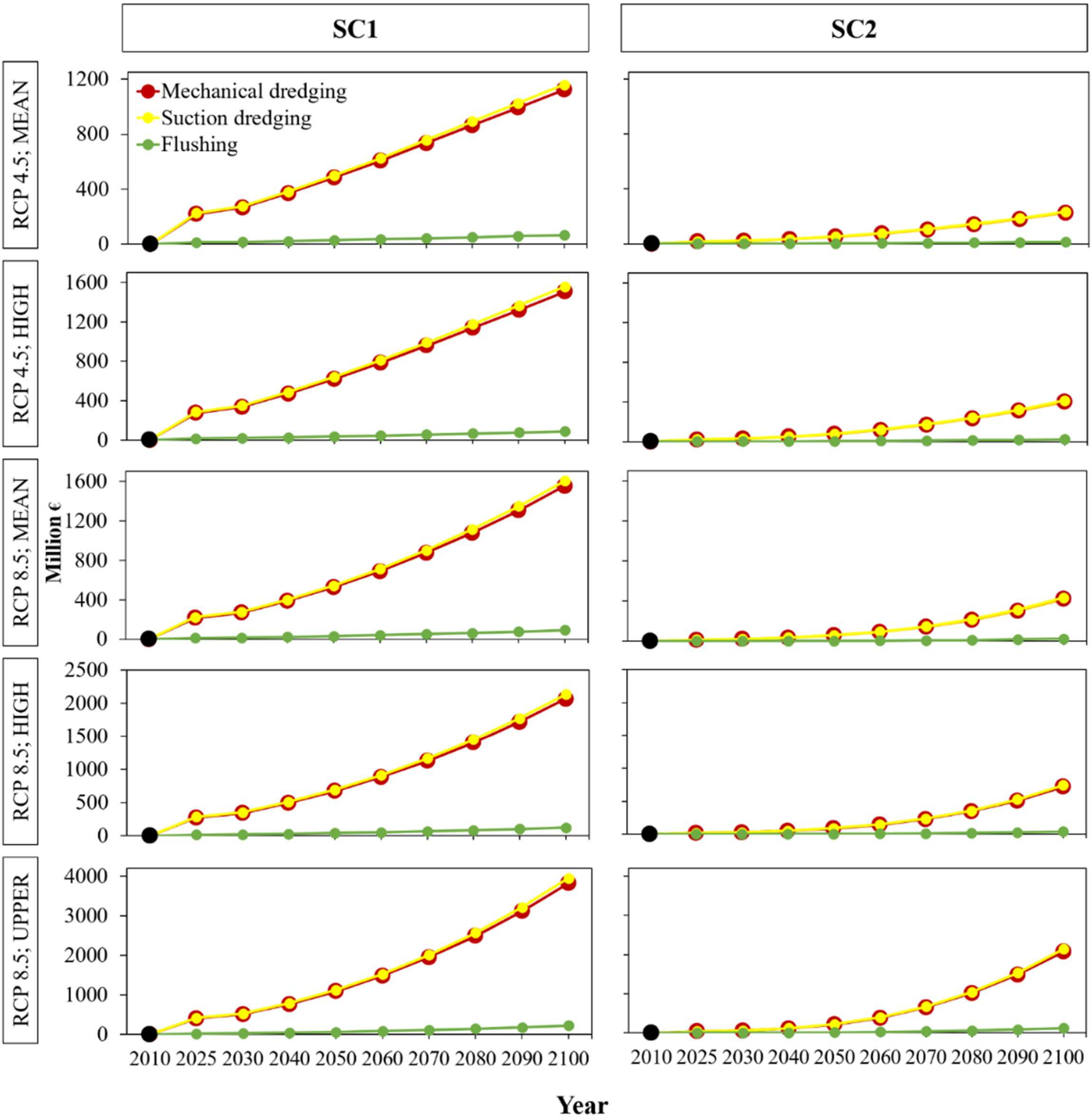
SC1
SC2
RCP 4.5; MEAN
RCP 4.5; HIGH
RCP 8.5; MEAN
RCP 8.5; HIGH
RCP 8.5; UPPER
Mechanical dredging
Suction dredging
Flushing
Million €
Year
2010 2025 2030 2040 2050 2060 2070 2080 2090 2100

890

Supplementary Table 1. Published functions considered to assess the relationship between soil bulk density (BD, g/cm^3) and organic matter (OM, g/g soil).

Function	References*
$\ln(BD) = -2.31 - 1.079 \times \ln(OM) - 0.113 \times [\ln(OM)^2]$	Federer (1983)
$\ln(BD) = -2.39 - 1.316 \times \ln(OM) - 0.167 \times [\ln(OM)^2]$	Huntington et al., (1989)
$\ln(BD) = -1.81 - 0.892 \times \ln(OM) - 0.092 \times [\ln(OM)^2]$	Prevost (2004)
$BD = (1.111 \times 1.450) / (1.450 \times OM) + 0.111 \times (1 - OM)$	Federer et al., (1993)
$BD = (1.244 \times 1.640) / (1.640 \times OM) + 0.244 \times (1 - OM)$	Post and Kwon (2000)
$BD = (1.120 \times 1.400) / (1.400 \times OM) + 0.120 \times (1 - OM)$	Tremblay et al., (2002)
$BD = (1.159 \times 1.561) / (1.561 \times OM) + 0.159 \times (1 - OM)$	Prevost (2004)
$BD = (1.111 \times 1.767) / (1.767 \times OM) + 0.111 \times (1 - OM)$	Périé and Ouimet (2008)
$BD = -1.977 + 4.105 \times OM - 1.229 \times \ln(OM) - 0.103 \times [\ln(OM)^2]$	Périé and Ouimet (2008)
$BD = -0.970 + 1.033 \times OM - 0.912 \times \ln(OM) - 0.095 \times [\ln(OM)^2]$	This study: modified from Périé and Ouimet (2008)

***References:**

Federer, C.A., 1983. Nitrogen mineralization and nitrification: depth variation in four New England forest soils. Soil Sci. Soc. Am. J. 47, 1008–1014. DOI

Federer, C.A., Turcotte, D.E., Smith, C.T., 1993. The organic fraction-bulk density relationship and the expression of nutrient content in forest soils. Can. J. For. Res. 23, 1026–1032. DOI

Huntington, T.G., Johnson, C.E., Johnson, A.H., Siccama, T.G., Ryan, D.F., 1989. Carbon, organic matter, and bulk density relationships in a forested Spodosol. Soil Sci. 148, 380–386.

Perie, C., Ouimet, R., 2008. Organic carbon, organic matter and bulk density relationships in boreal forest soils. Canandian Journal of Soil Science 88, 315–325. DOI

Post, W.M., Kwon, K.C., 2000. Soil carbon sequestration and land-use change: processes and potential. Global Change Biology 6, 317–327. DOI

Prévost, M., 2004. Predicting soil properties from organic matter content following mechanical site preparation of forest soils. Soil Science Society of America Journal 68, 943–949. DOI

Tremblay, S., Ouimet, R., Houle, D., 2002. Prediction of organic carbon content in upland forest soils of Quebec, Canada. Canadian Journal of Forest Research 32, 903–914. DOI

Supplementary Table 2. Full list of variables initially included in the organic matter model. The quadratic component of all continuous variables was also included.

Variables initially included in the model	Source
1- Location of the sample point (north, south)	GIS database
2- Surface elevation of 2010 (m) 3- Surface elevation of 2010 (interpolated) (m)	DEM 2010
4- Distance to the Ebro River (m) 5- Distante to the mouth (m) 6- Distance to the old mouth (m) 7- Distance to the coastline (m) 8- Distance to the northern border (m) 9- Distance to the southern border (m) 10- Distance to the inner border (m) 11- Distance to the nearest coastal lagoon (m)	GIS database
12- Predicted soil salinity (dS/m)	Genua-Olmedo et al., (2016)
13- Clay presence 14- Silt presence 15- Sand presence 16- Gravel presence 17- Peat presence 18- Block presence 19- Pebbles presence	ICGC, 2006; 1:50,000 scale sheets number 522-523, 547-548

Supplementary Table 3. SLR scenarios modelled (m): RCP 4.5 (stabilization) and RCP 8.5 (increasing radiative forcing) were obtained from the mean and high values of the AR5 IPCC projections, and the upper limit SLR, from Jevrejeva et al., (2014).

	RCP 4.5		**RCP 8.5**		
Year	Mean SLR	High SLR	Mean SLR	High SLR	Upper Limit SLR
2025	0.103	0.130	0.101	0.129	0.190
2030	0.126	0.159	0.126	0.160	0.240
2040	0.174	0.221	0.182	0.232	0.363
2050	0.228	0.291	0.248	0.317	0.514
2060	0.285	0.369	0.324	0.415	0.697
2070	0.345	0.451	0.411	0.530	0.918
2080	0.407	0.536	0.508	0.660	1.173
2090	0.467	0.622	0.614	0.807	1.468
2100	0.528	0.710	0.731	0.971	1.801

Supplementary Table 4. Estimation of flooded area, sediment volume deficit and mass, mean soil salinity (ECe), mean rice productivity index (RPI) and mean income under the considered SLR scenarios for SC1 and SC2, rice fields (210 km^2) and in the other deltaic areas (80 km^2). SC1 considers the total sediment volume deficit needed to maintain deltaic surface elevation relative to mean sea level as in the reference state (*i.e.* 2010), and SC2 considered the total sediment volume deficit needed to raise inundated areas just enough to compensate the RCP SLR scenario. The table continues in next page.

		Flooded area * (km^2)		Sediment volume deficit (10^6 m^3) Scenario 1 (SC1)		Sediment volume deficit (10^6 m^3) Scenario 2 (SC2)		Sediment mass deficit (10^6 tonnes) Scenario 1 (SC1)		Sediment mass deficit (10^6 tonnes) Scenario 2 (SC2)		Scenario 2 (SC2)**		
	Year	Rice fields	Deltaic areas	Rice fields	Deltaic areas	Rice fields	Deltaic areas	Rice fields	Deltaic areas	Rice fields	Deltaic areas	ECe (dS/m)	RPI (%)	Income (€/ha)
RCP 4.5 Mean SLR	2025	9.26	2.84	23.9	6.62	1.72	0.41	25.2	7.17	1.70	0.40	5.70	60.3	2347
	2030	12.3	3.87	29.2	8.09	2.26	0.55	30.8	8.76	2.23	0.54	5.75	60.1	2345
	2040	19.7	6.60	40.5	11.21	3.65	0.94	42.7	12.1	3.63	0.92	5.85	59.6	2339
	2050	27.8	11.0	53.0	14.66	5.61	1.56	55.9	15.9	5.60	1.53	5.96	59.1	2333
	2060	36.1	16.2	66.2	18.32	8.15	2.51	69.8	19.8	8.18	2.46	6.07	58.6	2327
	2070	45.4	20.1	80.2	22.20	11.4	3.79	84.6	24.0	11.4	3.73	6.18	58.1	2320
	2080	55.4	23.3	94.5	26.16	15.3	5.30	99.7	28.3	15.4	5.24	6.29	57.6	2314
	2090	65.4	26.2	108	30.03	19.7	6.97	114	32.5	19.9	6.92	6.39	57.1	2309
	2100	76.0	29.3	122	33.99	24.8	8.86	130	36.8	25.3	8.83	6.48	56.7	2304
RCP 4.5 High SLR	2025	12.9	4.06	30.1	8.35	2.36	0.58	31.8	9.04	2.34	0.57	5.76	60.0	2344
	2030	17.2	5.60	36.9	10.2	3.16	0.80	38.9	11.1	3.14	0.78	5.82	59.8	2341
	2040	26.9	10.4	51.4	14.2	5.34	1.47	54.3	15.4	5.34	1.44	5.95	59.2	2333
	2050	37.1	16.7	67.7	18.7	8.47	2.63	71.4	20.3	8.51	2.58	6.08	58.5	2326
	2060	49.1	21.4	85.6	23.7	12.8	4.34	90.4	25.7	12.9	4.28	6.22	57.5	2313
	2070	62.7	25.5	105	29.0	18.4	6.50	111	31.4	18.7	6.44	6.36	58.0	2320
	2080	77.4	29.6	125	34.5	25.5	9.11	131	37.4	26.0	9.08	6.49	56.6	2303
	2090	91.6	33.7	144	40.0	33.9	12.1	153	43.3	34.6	12.1	6.60	56.1	2297
	2100	104	37.7	165	45.7	43.6	15.5	174	49.5	44.7	15.6	6.71	55.6	2291

RCP 8.5 Mean SLR	2025	9.14	2.80	23.5	6.52	1.69	0.40	24.8	7.06	1.66	0.39	5.70	60.3	2347
	2030	12.4	3.92	29.3	8.11	2.27	0.56	30.9	8.79	2.24	0.54	5.75	60.1	2344
	2040	20.9	7.15	42.4	11.7	3.91	1.02	44.7	12.7	3.89	1.00	5.76	59.5	2338
	2050	30.9	13.0	57.6	16.0	6.45	1.86	60.8	17.3	6.46	1.82	6.00	58.9	2330
	2060	41.9	18.9	75.2	20.8	10.2	3.31	79.4	22.6	10.2	3.25	6.14	58.2	2322
	2070	56.1	23.5	95.5	26.4	15.5	5.42	101	28.6	15.7	5.35	6.29	57.5	2314
	2080	72.4	28.2	118	32.6	23.0	8.20	124	35.4	23.4	8.16	6.45	56.8	2305
	2090	90.4	33.4	143	39.5	33.0	11.8	151	42.8	33.8	11.8	6.59	56.1	2297
	2100	107	38.5	170	47.0	46.1	16.3	179	50.9	47.3	16.5	6.73	55.5	2289
RCP 8.5 High SLR	2025	12.9	4.06	30.0	8.3	2.34	0.58	31.6	8.99	2.31	0.56	5.76	60.1	2344
	2030	17.5	5.71	37.2	10.3	3.21	0.82	39.3	11.2	3.18	0.80	5.82	59.7	2340
	2040	28.5	11.5	53.9	14.9	5.77	1.62	56.9	16.2	5.77	1.59	5.97	59.1	2332
	2050	40.8	18.4	73.5	20.4	9.8	3.15	77.6	22.1	9.8	3.10	6.13	58.3	2323
	2060	56.9	23.7	96.4	26.7	15.8	5.53	102	28.9	16.0	5.46	6.30	57.5	2314
	2070	76.2	29.3	123	34.1	24.9	8.90	130	36.9	25.4	8.87	6.48	56.7	2304
	2080	97.4	35.5	153	42.4	37.9	13.5	162	46.0	38.8	13.6	6.65	55.8	2294
	2090	117	41.2	187	51.9	55.7	19.6	198	56.2	57.2	19.9	6.81	55.1	2285
	2100	135	45.3	226	62.4	78.6	27.1	238	67.6	80.9	27.8	6.94	54.4	2277
RCP 8.5 Upper Limit SLR	2025	22.0	7.66	44.1	12.2	4.17	1.10	46.5	13.2	4.15	1.07	5.88	59.5	2337
	2030	29.7	12.2	55.8	15.4	6.11	1.74	58.9	16.7	6.11	1.70	5.98	59.0	2331
	2040	48.1	21.0	84.2	23.3	12.4	4.20	88.9	25.3	12.5	4.14	6.21	57.9	2319
	2050	73.4	28.5	119	33.0	23.5	8.39	126	35.8	23.9	8.36	6.46	56.8	2305
	2060	103	37.2	162	44.8	42.1	14.9	171	48.6	43.2	15.1	6.69	55.6	2291
	2070	130	44.1	213	59.0	70.8	24.6	225	63.9	72.8	25.1	6.90	54.6	2279
	2080	153	48.4	272	75.4	111	37.1	288	81.7	114	38.4	7.07	53.8	2269
	2090	171	50.7	341	94.4	162	52.5	360	102.3	168	54.7	7.21	53.1	2261
	2100	187	52.9	418	116	227	70.6	442	125.5	235	73.9	7.32	52.6	2255

* Surface: Ebro Delta = 320 km^2, rice fields = 210 km^2, other deltaic areas = 80 km^2.

** SC1 refers to the reference state (year 2010): ECe = 5.53 dS/m; RPI = 61.2 %; income = 2359.38 €/ha. In SC1, RPI is constant along time for a given pixel since elevation is maintained as in the reference state, for more details on RPI see (Genua-Olmedo et al., 2016).

		Mechanical dredging (Millions €)								Suction dredging (Millions €)								Flushing (Millions €)			
		Scenario 1 (SC1)				Scenario 2 (SC2)				Scenario 1 (SC1)				Scenario 2 (SC2)				Scenario 1 (SC1)		Scenario 2 (SC2)	
		Rice fields		Deltaic areas		Rice fields		Deltaic areas		Rice fields		Deltaic areas		Rice fields		Deltaic areas		Rice fields	Deltaic areas	Rice fields	Deltaic areas
	Year	Min	Max	Min	Max	Min	Max	Min	Max	Min	Max	Min	Max	Min	Max	Min	Max	Unique			
RCP 4.5 Mean SLR	2025	206	232	57	64	15	17	3.5	4.0	108	344	30	95	7.8	25	1.9	5.9	13	3.6	0.9	0.2
	2030	251	283	70	78	19	22	4.8	5.4	132	421	36	117	10	33	2.5	8.1	16	4.4	1.2	0.3
	2040	348	393	96	109	31	35	8.1	9.1	182	583	50	161	16	53	4.2	14	22	6.1	2.0	0.5
	2050	455	514	126	142	48	54	13	15	238	763	66	211	25	81	7.1	23	29	7.9	3.0	0.8
	2060	569	642	157	178	70	79	21	24	298	953	82	264	37	117	11	36	36	9.9	4.4	1.4
	2070	689	778	191	215	98	110	32	36	361	1154	100	320	51	164	17	55	43	12	6.1	2.0
	2080	812	916	225	253	131	147	46	51	425	1360	118	377	69	220	24	76	51	14	8.2	2.9
	2090	933	1052	258	291	169	191	60	68	488	1561	135	432	89	283	31	100	59	16	11	3.8
	2100	1056	1191	292	330	213	241	76	86	552	1767	153	490	112	357	40	128	66	18	13	4.8
RCP 4.5 High SLR	2025	259	292	72	81	20	23	5.0	5.6	136	434	38	120	11	34	2.6	8.4	16	4.5	1.3	0.3
	2030	317	358	88	99	27	31	6.9	7.8	166	531	46	147	14	46	3.6	11	20	5.5	1.7	0.4
	2040	442	499	122	138	46	52	12	14	231	741	64	205	24	77	6.6	21	28	7.7	2.9	0.8
	2050	582	657	161	182	73	82	23	26	305	974	84	270	38	122	12	38	37	10	4.6	1.4
	2060	736	830	204	230	109	124	37	42	385	1233	107	341	58	184	20	63	46	13	6.9	2.3
	2070	900	1015	249	281	158	179	60	63	471	1507	130	417	83	265	29	94	57	16	9.9	3.5
	2080	1070	1207	297	335	219	247	78	88	560	1793	155	497	115	367	41	131	67	19	14	4.9

2090	1242	1401	344	388	291	328	104	117	650	2080	180	576	152	488	54	174	78	22	18	6.5
2100	1418	1599	393	443	375	423	133	150	742	2374	206	658	196	628	70	223	89	25	24	8.3

Supplementary Table 5. Estimated costs associated to sediment extraction and transport for mechanical dredging, suction dredging and flushing techniques under the simulated SLR for SC1 and SC2 in the rice fields (210 km^2) and in the other deltaic areas (80 km^2). SC1, considers the total sediment volume deficit needed to maintain deltaic surface elevation relative to mean sea level as in the reference state (*i.e.* 2010), and SC2 considers the total sediment volume deficit needed to raise inundated areas just enough to compensate the RCP SLR scenario. The cost is the sum of the cost of extraction which varied on the water depth of the sediment extraction, being minimum (water depth < 5 m) and maximum (water depth > 5 m), and the cost of the extra transport which only considered the pipeline. See Table 1 for more details. The table continues in next page.

RCP 8.5 Mean SLR	2025	202	228	56	63	15	16	3.5	3.9	106	339	29	94	7.6	24	1.8	5.8	13	3.5	0.9	0.2
	2030	252	284	70	79	20	22	4.8	5.4	132	422	37	117	10	33	2.5	8.0	16	4.4	1.2	0.3
	2040	364	411	101	114	34	38	8.8	9.9	191	610	53	169	18	56	4.6	15	23	6.3	2.1	0.6
	2050	496	559	137	155	56	63	16	18	259	830	72	230	30	92	8.4	27	31	8.6	3.5	1.0
	2060	647	730	179	202	87	99	28	32	339	1083	94	300	46	146	15	48	41	11	5.5	1.8
	2070	821	926	227	256	134	151	47	53	430	1375	119	380	70	224	24	78	52	14	8.4	2.9
	2080	1014	1144	281	317	198	223	71	80	531	1698	147	470	104	331	37	118	64	18	12	4.
	2090	1227	1384	340	383	284	321	101	114	642	2054	178	569	149	476	53	170	77	21	18	6.4
	2100	1459	1646	404	456	397	447	140	158	764	2444	212	677	208	664	73	235	92	25	25	8.8
RCP 8.5 High SLR	2025	258	291	71	80	20	23	4.9	5.6	135	431	37	119	11	34	2.6	8.3	16	4.5	1.3	0.
	2030	320	361	89	100	28	31	7.0	7.9	167	536	46	148	14	46	3.7	12	20	5.6	1.7	0.
	2040	464	523	128	145	50	56	14	16	243	776	67	215	26	83	7.3	23	29	8.1	3.1	0.
	2050	632	713	175	198	84	95	27	31	331	1059	92	293	44	141	14	45	40	11	5.3	1.
	2060	829	935	230	259	136	154	48	54	434	1388	120	384	71	228	25	80	52	14	8.5	3.
	2070	1058	1194	293	331	214	242	77	86	554	1772	153	491	112	359	40	128	66	18	14	4.
	2080	1318	1487	365	412	326	368	116	131	690	2207	191	611	171	546	61	194	83	23	21	7.
	2090	1612	1818	446	503	479	540	168	189	843	2699	233	748	251	802	88	282	101	28	30	11
	2100	1939	2187	537	606	676	762	233	262	1015	3247	281	899	354	1132	122	390	122	34	42	15
RCP 8.5 Upper	2025	379	428	105	118	36	40	9	11	198	635	55	179	19	60	4.9	16	24	6.6	2.3	0.6
	2030	480	541	133	150	53	59	15	17	251	803	70	222	27	88	7.8	25	30	8.3	3.3	0.9
	2040	724	817	201	226	107	120	36	41	379	1213	105	336	56	179	19	60	45	13	6.7	2.3

2050	1026	1158	284	321	202	228	72	81	537	1719	149	476	106	339	38	121	64	18	13	4.5
2060	1393	1571	386	435	362	409	129	145	729	2332	202	646	190	607	67	215	87	24	23	8.1
2070	1833	2068	508	573	609	687	211	238	959	3070	266	850	319	1020	111	354	115	32	38	13
2080	2343	2643	649	732	950	1072	319	360	1226	3923	340	1086	497	1591	167	535	147	41	60	20
2090	2932	3307	812	916	1397	1575	452	509	1534	4910	425	1359	731	2338	236	756	184	51	87	28
2100	3597	4058	996	1124	1950	2199	607	685	1882	6024	521	1668	1020	3264	318	1016	226	63	122	38

Supplementary Table 6. Economic cost-benefit analysis. The net benefit for a given scenario was the difference between the rice income with the nature-based adaptation (sediment deposition), and the rice income without adaptation (without sediment deposition). The cost was calculated by the cost of sediment extraction and transport based on our estimations of sediment volume deficit (see Supplementary Table 5). The economic cost-benefit analysis was the difference between the benefit and the cost. SC1, considers the total sediment volume deficit needed to maintain deltaic surface elevation relative to mean sea level as in the reference state (*i.e.* 2010), and SC2 considers the total sediment volume deficit needed to raise inundated areas just enough to compensate the RCP SLR scenario.

		Income (€/ha)					Cost-benefit (Million €)					
		With adaptation			Net benefit		Mechanical dredging		Suction dredging		Flushing	
	Year	SC1	SC2	Without adaptation	SC1	SC2	SC1	SC2	SC1	SC2	SC1	SC2
RCP 4.5 Mean SLR	2025	2359	2347	2343	16	3.78	-219	-16	-226	-16	-13	-0.8
	2030	2359	2344	2339	20	4.60	-267	-20	-276	-21	-16	-1.1
	2040	2359	2338	2332	27	6.07	-370	-33	-382	-34	-21	-1.9
	2050	2359	2332	2325	34	7.16	-484	-51	-500	-53	-28	-2.8
	2060	2359	2326	2317	42	9.37	-605	-74	-625	-77	-35	-4.2
	2070	2359	2320	2307	52	12.7	-732	-104	-756	-107	-42	-5.8
	2080	2359	2314	2298	61	16.2	-863	-139	-891	-144	-50	-7.9
	2090	2359	2308	2288	71	20.3	-991	-180	-1023	-186	-57	-11
	2100	2359	2303	2279	80	24.6	-1122	-226	-1158	-234	-64	-12
RCP 4.5 High SLR	2025	2359	2344	2339	20	4.13	-275	-21	-285	-22	-16	-1.2
	2030	2359	2341	2335	24	5.48	-337	-29	-348	-30	-19	-1.6
	2040	2359	2333	2326	33	6.70	-470	-49	-485	-50	-27	-2.8
	2050	2359	2326	2316	43	9.83	-619	-77	-639	-80	-36	-4.4
	2060	2359	2313	2296	62	16.5	-782	-116	-808	-121	-45	-6.6
	2070	2359	2311	2284	74	25.6	-956	-168	-987	-173	-55	-9.4
	2080	2359	2303	2277	82	25.2	-1137	-232	-1175	-240	-65	-13
	2090	2359	2297	2263	96	33.0	-1319	-309	-1363	-319	-76	-17
	2100	2359	2291	2248	111	42.7	-1506	-398	-1556	-411	-87	-23

RCP 8.5 Mean SLR	2025	2359	2347	2343	16	3.97	-215	-15	-222	-16	-13	-0.8
	2030	2359	2344	2340	20	4.57	-268	-21	-277	-21	-16	-1.1
	2040	2359	2338	2332	28	6.33	-387	-36	-400	-37	-22	-2.0
	2050	2359	2330	2322	37	8.54	-527	-59	-544	-61	-30	-3.3
	2060	2359	2322	2310	49	12.5	-687	-93	-710	-96	-40	-5.2
	2070	2359	2314	2297	62	17.0	-872	-142	-901	-147	-51	-8.0
	2080	2359	2305	2281	78	23.9	-1077	-210	-1113	-217	-62	-12
	2090	2359	2297	2264	96	33.5	-1303	-302	-1346	-312	-75	-17
	2100	2359	2289	2244	115	44.9	-1550	-421	-1602	-435	-90	-24
RCP 8.5 High SLR	2025	2359	2344	2340	20	4.22	-274	-21	-283	-22	-16	-1.2
	2030	2359	2340	2335	24	5.32	-340	-29	-351	-30	-20	-1.6
	2040	2359	2332	2324	35	7.90	-493	-53	-509	-54	-28	-2.9
	2050	2359	2323	2312	47	10.8	-672	-89	-694	-92	-39	-5.1
	2060	2359	2314	2297	62	16.6	-881	-145	-910	-149	-51	-8.2
	2070	2359	2304	2278	82	25.7	-1124	-227	-1161	-235	-64	-13
	2080	2359	2294	2256	103	37.5	-1400	-346	-1446	-358	-81	-20
	2090	2359	2285	2231	128	53.6	-1712	-508	-1768	-525	-98	-29
	2100	2359	2277	2202	158	75.4	-2060	-717	-2128	-741	-118	-40
RCP 8.5 Upper Limit SLR	2025	2359	2337	2330	29	6.68	-403	-38	-416	-39	-23	-2.2
	2030	2359	2331	2323	36	8.22	-510	-56	-526	-57	-29	-3.1
	2040	2359	2319	2305	54	13.3	-769	-113	-795	-117	-44	-6.4
	2050	2359	2305	2281	78	23.4	-1090	-215	-1126	-222	-62	-13
	2060	2359	2291	2250	109	41.0	-1480	-385	-1528	-398	-85	-22
	2070	2359	2279	2211	148	68.2	-1947	-647	-2011	-668	-112	-37
	2080	2359	2269	2162	197	107.0	-2489	-1009	-2570	-1042	-143	-58
	2090	2359	2261	2103	257	158.3	-3114	-1483	-3217	-1531	-179	-84
	2100	2359	2255	2031	328	223.6	-3821	-2070	-3946	-2137	-219	-117

Supplementary Table 7. Values of flooded area, sediment volume deficit and mass considering a subsidence rate of 2.7 mm/yr under SLR scenarios for SC1 and SC2, rice fields (210 km^2) and in the other deltaic areas (80 km^2). SC1 considers the total sediment volume deficit needed to maintain deltaic surface elevation relative to mean sea level as in the reference state (i.e. 2010), and SC2 considered the total sediment volume deficit needed to raise inundated areas just enough to compensate the RCP SLR scenario. The table continues in next page**.**

		Flooded area * (km^2)		Sediment volume deficit (10^6 m^3)				Sediment mass deficit (10^6 tonnes)			
				Scenario 1 (SC1)		Scenario 2 (SC2)		Scenario 1 (SC1)		Scenario 2 (SC2)	
	Year	Rice fields	Deltaic areas	Rice fields	Deltaic areas	Rice fields	Deltaic areas	Rice fields	Deltaic areas	Rice fields	Deltaic areas
RCP 4.5 Mean SLR	2025	14.9	5.91	33.3	9.23	5.34	1.26	35.2	10.01	5.12	1.18
	2030	20.5	8.09	41.8	11.6	6.44	1.58	44.1	12.6	6.23	1.49
	2040	31.9	14.9	59.3	16.4	9.38	2.57	62.6	17.8	9.20	2.46
	2050	43.9	20.8	78.0	21.6	13.5	4.19	82.4	23.5	13.4	4.05
	2060	57.6	25.1	97.5	27.0	18.8	6.28	102	29.3	18.8	6.12
	2070	72.4	29.4	117	32.7	25.6	8.84	124	35.4	25.8	8.68
	2080	87.3	33.7	138	38.4	33.8	11.8	138	38.4	34.3	11.7
	2090	100	37.7	159	44.0	43.1	15.2	167	47.6	43.9	15.0
	2100	112	41.2	179	49.7	53.8	18.8	189	53.8	54.9	18.8
RCP 4.5 High SLR	2025	19.0	7.49	39.6	11.0	6.13	1.48	41.8	11.9	5.92	1.40
	2030	25.5	10.7	49.4	13.7	7.62	1.95	52.2	14.9	7.42	1.85
	2040	38.8	18.7	70.2	19.5	11.6	3.46	74.2	21.1	11.5	3.33
	2050	54.2	24.1	92.7	25.7	17.3	5.74	97.9	27.9	17.3	5.58
	2060	71.7	29.2	116	32.4	25.2	8.73	123	35.1	25.5	8.57
	2070	90.1	34.5	142	39.5	35.5	12.4	150	42.8	36.0	12.3
	2080	106	39.6	168	46.7	48.1	16.8	178	50.6	49.0	16.8
	2090	120	43.2	194	54.0	62.4	21.8	205	58.5	63.8	21.3
	2100	133	46.1	221	61.4	78.6	27.2	233	66.5	80.5	27.5

RCP 8.5 Mean SLR	2025	14.6	5.81	32.9	9.13	5.29	1.24	34.8	9.90	5.07	1.16
	2030	20.6	8.16	41.8	11.6	6.45	1.58	44.2	12.6	6.24	1.49
	2040	33.1	15.6	61.2	17.0	9.75	2.71	64.6	18.4	9.57	2.59
	2050	47.2	21.9	82.7	22.9	14.6	4.66	87.3	24.9	14.5	4.51
	2060	64.1	27.0	106	29.6	21.7	7.38	112	32.0	21.7	7.21
	2070	83.5	32.6	133	36.9	31.6	11.0	140	39.9	31.9	10.9
	2080	102	38.4	161	44.9	44.7	15.7	170	48.6	45.5	15.6
	2090	120	43.1	192	53.5	61.4	21.4	203	57.9	62.7	21.5
	2100	136	46.5	226	62.7	81.6	28.1	238	67.9	83.7	28.5
RCP 8.5 High SLR	2025	18.9	7.42	39.4	10.9	6.11	1.48	41.6	11.8	5.89	1.39
	2030	25.8	10.9	49.8	13.8	7.68	1.96	52.5	14.9	7.47	1.87
	2040	40.4	19.4	72.7	20.1	12.2	3.68	76.8	21.8	12.1	3.55
	2050	58.4	25.4	98.6	27.4	19.1	6.41	104	29.6	19.1	6.25
	2060	79.8	31.5	128	35.4	29.4	10.2	134	38.4	29.7	10.1
	2070	102	38.1	160	44.6	44.2	15.5	169	48.3	45.0	15.4
	2080	121	43.6	197	54.7	63.9	22.3	208	59.2	65.3	22.4
	2090	140	47.5	237	65.9	89.1	30.6	250	71.4	91.5	31.0
	2100	155	50.0	281	78.2	120	40.3	297	84.7	123	41.2
RCP 8.5 Upper Limit SLR	2025	28.2	12.4	53.5	14.8	8.32	2.18	56.5	16.1	8.12	2.08
	2030	37.6	18.1	68.3	18.9	11.2	3.29	72.1	20.5	11.1	3.16
	2040	61.6	26.3	103	28.6	20.5	6.94	108	31.0	20.6	6.78
	2050	91.6	34.9	144	40.0	36.5	12.8	152	43.4	37.0	12.7
	2060	120	43.1	193	53.6	61.6	21.5	204	58.1	63.0	21.6
	2070	145	48.4	250	69.6	98.0	33.4	264	75.4	100	34.0
	2080	165	51.2	316	87.7	145	48.2	334	95.1	150	49.4
	2090	181	53.4	391	108	206	65.8	412	117	213	67.7
	2100	194	55.7	474	131	279	86.3	501	142	289	89.1

Supplementary Figure 1. Evolution of the flooded area in 2050, 2070 and 2100 for the considered SLR scenarios: mean and high RCP 4.5, and mean, high and upper limit RCP 8.5. See materials and methods for RCP description.

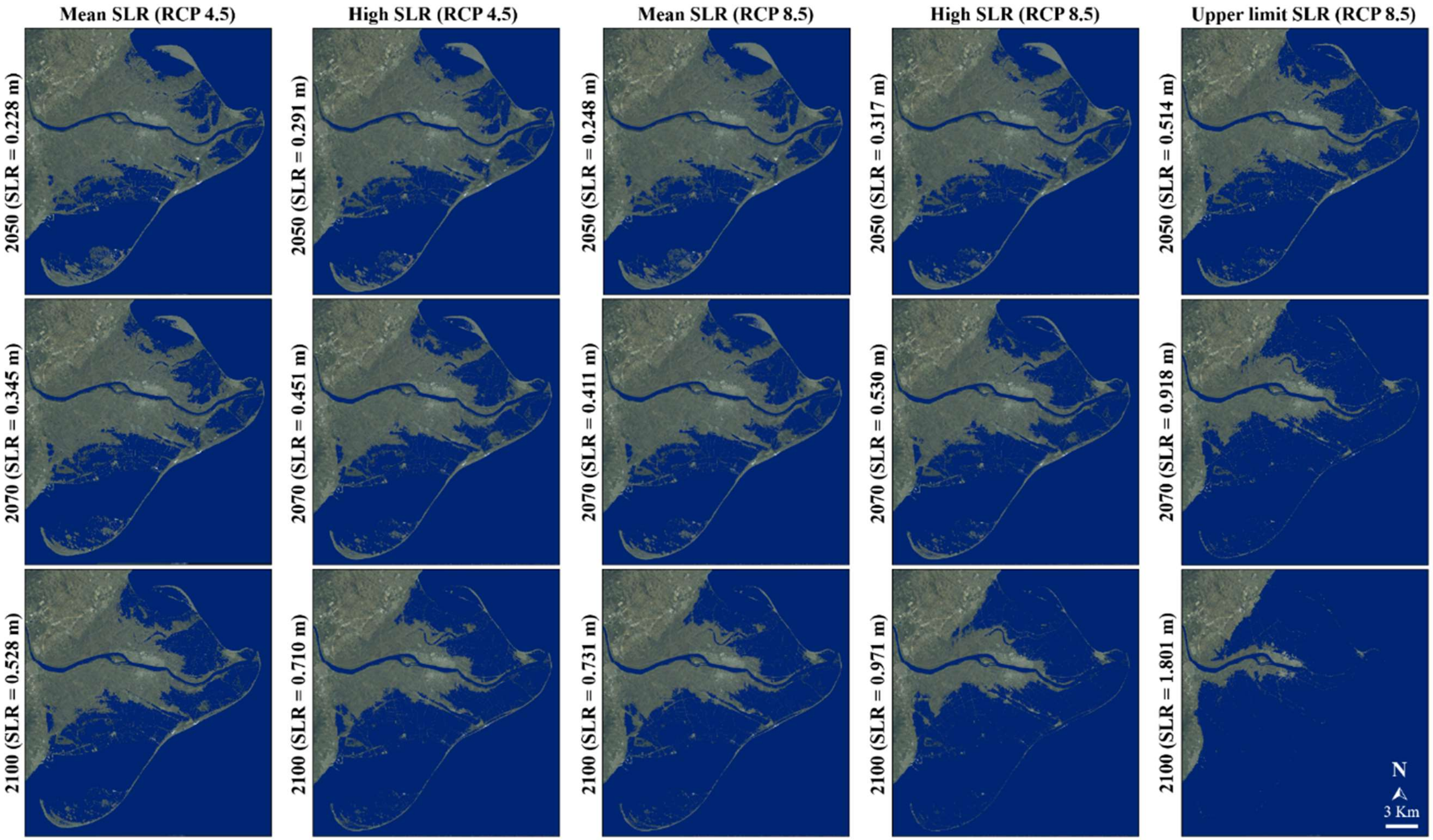

Supplementary Figure 2. Soil bulk density (a) and soil organic matter content (b) distribution maps in the Ebro Delta. To convert BD g/cm^3 units to kg/m^3, multiply per 1000.